Spatial variability in the isotopic composition of rainfall in a small headwater catchment and its effect on hydrograph separation

Fischer, Benjamin M C ; van Meerveld, H J (Ilja) ; Seibert, Jan

Abstract: Isotope hydrograph separation (IHS) is a valuable tool to study runoff generation processes. To perform an IHS, samples of baseflow (pre-event water) and streamflow are taken at the catchment outlet. For rainfall (event water) either a bulk sample is collected or it is sampled sequentially during the event. For small headwater catchment studies, event water samples are usually taken at only one sampling location in or near the catchment because the spatial variability in the isotopic composition of rainfall is assumed to be small. However, few studies have tested this assumption. In this study, we investigated the spatiotemporal variability in the isotopic composition of rainfall and its effects on IHS results using detailed measurements from a small pre-alpine headwater catchment in Switzerland. Rainfall was sampled sequentially at eight locations across the 4.3 km2 Zwäckentobel catchment and stream water was collected in three subcatchments (0.15, 0.23, and 0.70 km2) during ten events. The spatial variability in rainfall amount, average and maximum rainfall intensity and the isotopic composition of rainfall was different for each event. There was no significant relation between the isotopic composition of rainfall and total rainfall amount, rainfall intensity or elevation. For eight of the ten studied events the temporal variability in the isotopic composition of rainfall was larger than the spatial variability in the rainfall isotopic composition. The isotope hydrograph separation results, using only one rain sampler, varied considerably depending on which rain sampler was used to represent the isotopic composition of event water. The calculated minimum pre-event water contributions differed up to 60%. The differences were particularly large for events with a large spatial variability in the isotopic composition of rainfall and a small difference between the event and pre-event water isotopic composition. Our results demonstrate that even in small catchments the spatial variability in the rainfall isotopic composition can be significant and has to be considered for IHS studies. Using data from only one rain sampler can result in significant errors in the estimated pre-event water contributions to streamflow.

DOI: https://doi.org/10.1016/j.jhydrol.2017.01.045

Fischer, Benjamin M C; van Meerveld, H J (Ilja); Seibert, Jan (2017). Spatial variability in the isotopic composition of rainfall in a small headwater catchment and its effect on hydrograph separation. Journal of Hydrology, 547:755-769.
DOI: https://doi.org/10.1016/j.jhydrol.2017.01.045

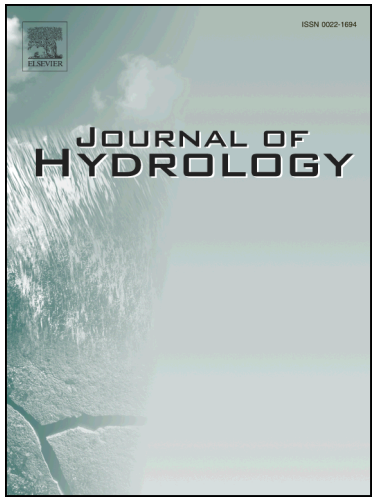

Research papers

Spatial variability in the isotopic composition of rainfall in a small headwater catchment and its effect on hydrograph separation

Benjamin M.C. Fischer, Ilja van Meerveld, Jan Seibert

PII: S0022-1694(17)30055-0
DOI: http://dx.doi.org/10.1016/j.jhydrol.2017.01.045
Reference: HYDROL 21784

To appear in: *Journal of Hydrology*

Received Date: 9 August 2016
Revised Date: 23 January 2017
Accepted Date: 24 January 2017

Please cite this article as: Fischer, B.M.C., van Meerveld, I., Seibert, J., Spatial variability in the isotopic composition of rainfall in a small headwater catchment and its effect on hydrograph separation, *Journal of Hydrology* (2017), doi: http://dx.doi.org/10.1016/j.jhydrol.2017.01.045

SPATIAL VARIABILITY IN THE ISOTOPIC COMPOSITION OF RAINFALL IN A SMALL HEADWATER CATCHMENT AND ITS EFFECT ON HYDROGRAPH SEPARATION

Benjamin M. C. Fischer[1], Ilja van Meerveld[1] and Jan Seibert[1,2]

[1] Department of Geography, University of Zurich, Winterthurerstrasse 190, CH-8057 Zurich, Switzerland Tel.: +41-44-63 55227, Fax.: +41-44-63 56841, corresponding author: benjamin.fischer@geo.uzh.ch

[2] Department of Earth Sciences, Uppsala University, Sweden

Keywords: isotope hydrograph separation, precipitation, headwater catchment, spatial variability, uncertainty

ABSTRACT

Isotope hydrograph separation (IHS) is a valuable tool to study runoff generation processes. To perform an IHS, samples of baseflow (pre-event water) and streamflow are taken at the catchment outlet. For rainfall (event water) either a bulk sample is collected or it is sampled sequentially during the event. For small headwater catchment studies, event water samples are usually taken at only one sampling location in or near the catchment because the spatial variability in the isotopic composition of rainfall is assumed to be small. However, few studies have tested this assumption. In this study, we investigated the spatiotemporal variability of the isotopic composition of rainfall and its effects on IHS results using detailed measurements from a small pre-alpine headwater catchment in Switzerland. Rainfall was sampled sequentially at eight locations across the 4.3 km^2 Zwäckentobel catchment and stream water was collected in three subcatchments (0.15, 0.23, and 0.7 km^2) during ten events. The spatial variability in rainfall amount, average and maximum rainfall intensity and the isotopic composition of rainfall was different for each the different event. There was no

significant relation between the isotopic composition of rainfall and total rainfall amount, rainfall intensity or elevation. For eight of the ten studied events the temporal variability in the isotopic composition of rainfall was larger than the spatial variability in the rainfall isotopic composition. The isotope hydrograph separation results, using only one rain sampler, varied considerably depending on which rain sampler was used to represent the isotopic composition of event water. The calculated minimum pre-event water contributions differed up to 60 %. The differences were particularly large for events with a large spatial variability in the isotopic composition of rainfall and a small difference between the event and pre-event water composition. Our results demonstrate that even in small catchments the spatial variability in the rainfall isotopic composition can be significant and has to be considered for IHS studies. Using data from only one rain sampler can result in significant errors in the estimated pre-event water contributions to streamflow.

1. INTRODUCTION

Two-component isotope hydrograph separation (IHS) is a well-established method to study runoff generation processes (Burns, 2002; Buttle, 1994; Klaus and McDonnell, 2013). IHS makes uses of the stable isotopes of water ($\delta^{18}O$ and $\delta^{2}H$) as conservative tracers to estimate how much rainfall (event water) and water that was stored in the catchment prior to the event (pre-event water) contributes to streamflow (Sklash et al., 1976). To be able to perform an IHS, a baseflow water sample is collected at the catchment outlet before the start of an event (to represent pre-event water) and streamflow samples are collected throughout the event. Krupa (2002) and Laquer (1990) list different ways to collect rain water samples. Sampling by hand (Hrachowitz et al., 2011; Roa-García and Weiler, 2010), integrated volume samplers (James and Roulet, 2009; Lyon et al., 2008; Pellerin et al., 2008; Smith et al., 1979; Vitvar and Balderer, 1997) and sequential samples for each volume of rain or at a fixed time step (Brown et al., 1999; Jordan, 1994; Kennedy et al., 1986; McDonnell et al., 1990; Penna et al., 2014) are most common in IHS studies. Field laser spectroscopes that measure the isotopic

composition of rainfall directly with a high temporal resolution open new possibilities for IHS studies, but are so far rarely used (Berman et al., 2009; Munksgaard et al., 2012; Tweed et al., 2016; von Freyberg et al., 2016).

IHS relies on a number of assumptions, as discussed by Buttle (1994) and Klaus and McDonnell (2013). One of the assumptions is that the isotopic signature of event and pre-event water are significantly different and that both are constant throughout the event, or that any spatiotemporal variation can be accounted for. Conventionally, it is assumed that the contribution from the vadose zone is negligible, or that the isotopic signature of soil water is similar to that of groundwater and that surface storage contributes minimally to the streamflow.

The isotopic composition of rainfall can change significantly during an event. McDonnell et al. (1990) highlighted the importance of considering this temporal variation in IHS studies and proposed different weighing techniques to account for the temporal variation in the isotopic composition of rainfall. Similarly, Laudon et al. (2002) proposed a technique to weigh snowmelt to account for the temporal variation in the isotopic composition of snowmelt in IHS. Almost all IHS studies now take the temporal variability in the isotopic composition of event water into account. Very few studies in small catchments have tested the assumption that the isotopic signature of rainfall is spatially uniform and assessed how this assumption affects the IHS results. The common practice in IHS studies for small headwater catchments (< 10 km^2) is to sample rain at one location and to assume that the effects of spatial variability are negligible for both rainfall (Goodrich et al., 1995) and its isotopic composition (McDonnell and Beven, 2014).

The spatial variability in the isotopic composition of rainfall has been studied for large catchments at monthly time scales using data from national (Delavau et al., 2015; Katsuyama et al., 2015; Schürch et al., 2003; Seeger and Weiler, 2014; Smith et al., 1979) and global

(Araguás-Araguás et al., 2000; Bowen and Good, 2015; Dansgaard, 1964; Hughes and Crawford, 2012) monitoring networks. Some of these large scale studies, have shown a relations between the isotopic composition of precipitation and elevation (Holko et al., 2012; Kern et al., 2014; McGuire and McDonnell, 2008; Tappa et al., 2016), temperature (Dansgaard, 1964; Holko et al., 2012; Schürch et al., 2003; Tappa et al., 2016) or rainfall amount (Dansgaard, 1964) were observed. Contrary, Holko et al. (2012) and Schürch et al. (2003) did not observe an amount effect using distributed rain samplers in Slovakia and Switzerland respectively.

The isotopic composition of the rainfall is also affected by canopy interception (Kato et al., 2013; Xu et al., 2014). Detailed studies on small scale spatial variability in the isotopic composition of throughfall, have shown a substantial spatiotemporal variability in the isotopic composition of throughfall at both the plot (Allen et al., 2015) and catchment scale (James and Roulet, 2009).

Only a few studies have looked at the spatial variability in the isotopic composition of rainfall during individual events at the small catchment scale (Lyon et al., 2009; McGuire et al., 2005). McGuire et al. (2005) quantified the spatial variability in the isotopic composition of rainfall across the 62 km^2 H. J. Andrews Lookout Creek catchment for three events in fall 2002 using 38 bulk samplers and observed significant spatial differences and an elevation effect. Lyon et al. (2009) used two sequential rain sampler locations (two bulk samplers and one incremental sampler) to assess the influence of the spatial and temporal variability in the isotopic composition of rainfall on the calculated pre-event water contribution to streamflow for one event in the 8.8 km^2 Upper Sabino research catchment in Arizona. They observed small differences in the isotopic composition of the incremental weighted rainfall and the bulk rainfall sample, but substantial differences between the two rainfall locations (Lyon et al., 2009). These results show that the spatial variability in the isotopic composition of rainfall may significantly affect hydrograph separation results and that this effect should be

studied in more detail. Therefore, we investigated the spatiotemporal variability in the isotopic composition of rainfall across a headwater catchment in Switzerland and determined the effect of the location of the rain sampler on IHS results for three tributary streams. Rainfall was measured and sampled at eight locations across the 4.3 km^2 Zwäckentobel catchment at 5 mm intervals and streamflow was sampled in three 0.15-0.7 km^2 tributary streams for ten different events. Here, we use these data to address the following questions:

(1) What is the spatial variability in rainfall and its isotopic composition across a small pre-alpine headwater catchment at the event time scale and is this variability related to total rainfall amount, rainfall intensity or elevation?

(2) Does the choice of the location of the sequential rainfall sampler affect the isotope hydrograph separation results, and if so, does this effect depend on event size?

2. METHODS

2.1 Study area

The Zwäckentobel catchment is a 4.3 km^2 pre-alpine headwater catchment, located 40 km south of Zurich in Switzerland (Figure 1). The climate is humid with a mean annual temperature of 6 °C. The mean annual precipitation is 2300 mm y^{-1}, of which half falls during the snow-free season (Jun-Oct). It rains approximately every second day. The mean annual actual evaporation is 300-400 mm y^{-1} (Menzel et al., 2007).

<Figure 1 here please>

Ten perennial streams drain the Zwäckentobel catchment (Figure 1a), of which WS04 (Erlenbach catchment; 0.7 km^2), WS10 (0.23 km^2) and WS19 (0.15 km^2) have been the subject of several previous studies (Fischer et al., 2016, 2015; Hegg et al., 2006; Rinderer et al., 2014). These mountain streams respond quickly to rainfall and baseflow levels are usually reached again within a day.

The geology of the Zwäckentobel catchment is composed of three different types of Tertiary flysch that consist of calcareous sedimentary layers of schist, marl and sandstone and is covered by shallow creeping gleysols (0.5-2.5 m). Land cover consists of forest (54 %), partly forested meadows (21 %) and meadows (24 %) (Fischer et al., 2015). All land cover types contain wetlands, covering approximately a quarter to half of the different subcatchments area.

2.2 Instrumentation and event sampling

We used the dataset of Fischer et al. (2016), who collected hydrometric and stable isotope data in subcatchments WS04, WS10, and WS19 for 13 rainfall events during the snow free period (Jun-Oct) of 2010 and 2011. An event was defined as a period with more than 0.2 mm h^{-1} of precipitation that resulted in an increase in stream water level of more than 0.01 m (a rainfall period occurring before the stream water level had returned to baseflow conditions was considered to be part of the same event). Three events from the Fischer et al. (2016) dataset were excluded from the analyses due to malfunctioning of some of the rain samplers and, thus, only data from ten events (numbered 1 to 6 and 9 to 12) were used for analysis in this study (Table 1, 2 and 3).

<Table 1 here please>

Rainfall was measured at 14 locations in open fields using tipping bucket rain gauges installed at 1.5 m above ground level. The rain gauges and were located on different transects and across different elevation classes (Figure 1a). Two of the rain gauges were situated in WS04 (WG-01; Ott Pluvio, OTT Hydrometrie AG, Switzerland and TB-14; Joss-Tognini tipping bucket, Lamprecht meteo, Germany, 0.2 mm per tip with the total number of tips recorded every 10 minutes). The other 12 rain gauges were distributed across the Zwäckentobel (Davis II tipping bucket; Davis Instruments Corp., USA with Odyssey data logger; Dataflow Systems, New Zealand, 0.2 mm per tip with the total number of tips recorded every 5 minutes). The differences between the different tipping buckets (assessed by

checking the tipping buckets in the field at the beginning and end of the summer season 2011) was less than 5 %. Wind also induces an under-catch of rainfall, which depends on the rainfall intensity and wind speed (Nešpor and Sevruk, 1999). Wind speed data was only available at WG-01 (Figure 1a), and therefore we could not correct the rainfall data for wind induced errors.

Eight rain gauges were equipped with a sequential rain sampler, which was adapted after Kennedy et al. (1979). The rain water was collected from the tipping bucket using two funnels and routed through a tube into the sampler, which containing twelve 100 ml glass jars (each representing 5 mm of rainfall). The sampling design was restricted by logistics because all samples needed to be collected within one day to avoid fractionation. Therefore, sequential rain samplers were not installed in the upper parts of WS04 and WS10 (Figure 1a).

<Table 2 here please>

The stream water level was measured at the outlets of WS04, WS10 and WS19. Discharge was measured at the outlet of WS04. Before each event, a baseflow grab sample was taken from each stream to characterize the pre-event water composition. Automatic samplers (ISCO 6712 with twenty-four 1 L-bottles and a Liquid Level Actuator, Teledyne Isco, USA) were used to collect stream water samples during the events. The automatic samplers were programmed so that once the stream water level rose by more than 0.01 m, six samples were collected at a 10 minutes time interval (generally representing the rising limb), and another 18 samples were collected every 60 minutes afterwards (Fischer et al., 2016). The number of samples for stable isotope analysis differed for each stream and event and ranged from 7 samples for short events up to 54 samples for long events (Table 3).

All water samples were analyzed at the stable isotope laboratory of the Department of Geography at the University of Zurich using a Cavity Ring-Down Spectroscope-Picarro L1102-i Liquid Analyzer (1st generation analyzer, Picarro Inc., 2008), following the

procedure of Penna et al. (2010). All stable isotope values are reported as δ-values in per mill (‰) relative to Vienna Standard Mean Ocean Water (VSMOW). The precision for the isotope analyses was < 0.1 ‰ for $\delta^{18}O$, and generally < 0.5 ‰ for $\delta^{2}H$. However, due to technical issues, the precision for $\delta^{2}H$ was > 1 ‰ for some of the samples, therefore only the $\delta^{18}O$ data were used for IHS analysis in this study. Based on the $\delta^{2}H$ and $\delta^{18}O$ values it can be assumed that none of the samples were subject to significant fractionation (Fischer et al., 2016).

<Table 3 here please>

2.3 Spatiotemporal variability in rainfall and its isotopic composition

For each event and each rainfall sampler, the rainfall data (mm 5 min^{-1} and mm 10 min^{-1}) were aggregated from the start of the event to the end of the event and for one hour to obtain event total rainfall and the 1-hour average rainfall intensity, respectively. Because the rainfall samplers were connected to the tipping buckets it was possible to assign the filling time for each 5 mm of rainfall. The median time it took for this 5 mm of precipitation to fall was 65 minutes (the 25^{th} and 75^{th} percentile were 30 and 130 minutes, respectively). For events 3, 4, 5 and 11, rainfall started at the same time at all of the rain gauges, while for events 1 and 6 there was more than one hour difference in the onset of the rainfall at the different rain gauges (Table 1). As the rainfall varied across the catchment, the actual time period over which each individual sample was collected (and thus the time over which the isotopic composition of rainfall was averaged) varied. The median difference in the start or end time of filling was 7.5 minutes (the 25^{th} and 75^{th} percentile were 0 and 20 minutes respectively). This difference in the timing for each sample was considered to be relatively small (compared to the 10-70 hour event length and median collection time of 65 min) and assumed to have only a minor effect on the observed spatial differences in the isotopic composition of rainfall during events.

To determine which rain gauge was most representative for the Zwäckentobel catchment, we calculated the mean relative difference (M_{RD}) for event total rainfall using the method of Vachaud et al. (1985):

$$M_{RD\,P\,j} = \frac{1}{n}\sum_{i=1}^{n}\frac{P_{j,i} - \overline{P}_i}{\overline{P}_i} \quad (1)$$

where $M_{RD\,P\,j}$ is the Mean Relative Difference for rain gauge *j*, $P_{j,i}$ is the rainfall measured at rain gauge *j* for event *i*, $\overline{P}_i$ is the mean rainfall for all rain gauges for event *i*, and *n* is the total number of events (n = 10). The mean relative difference of the event weighted mean isotopic composition of rainfall ($M_{RD\,^{18}O\,j}$) was calculated similarly.

To determine the origin of the air masses for the different rainfall events, a 96-h back trajectory analysis was performed using the hybrid single particle Lagrangian integrated trajectory model (HYSPLIT, Draxler and Rolph, 2012), with a calculation at an altitude 2000 meter above ground level.

2.4 Spatiotemporal variability in event water composition on hydrograph separation results

A two-component isotope hydrograph separation (IHS) was used to quantify the fraction of pre-event water f_{PE} (Eq. 2 and 3) in streamflow (Sklash et al., 1976) for the ten rainfall-runoff events.

$$Q_S = Q_E + Q_{PE} \quad (2)$$

$$f_{PE} = \frac{C_S - C_E}{C_{PE} - C_E} \quad (3)$$

where *C* describes the stable isotope composition [‰], Q the streamflow [l s^{-1}] and the subscripts *S, PE* and *E* represent streamflow, pre-event water (baseflow prior to the event) and event water (rainfall) respectively. The different temporal weighing techniques described by McDonnell et al. (1990) were used to account for the temporal variability in the event water composition: (I) weighted mean, (II) intensity mean, (III) incremental mean and (IV)

incremental intensity mean. For both the weighted mean (I) and the incremental weighted mean (III) the value of C_E was computed from the isotope values, δ_k [‰], observed at the kth sample during the event, weighted by the precipitation amount, P_k [mm] (Eq.4).

$$C_E = \frac{\sum_{k=1}^{m} P_k \delta_k}{\sum_{k=1}^{m} P_k} \quad (4)$$

The intensity mean (II) and the incremental intensity mean (IV) were computed similarly based on the rainfall intensity, I_k [mm h^{-1}] (Eq. 5). For the weighted mean all samples throughout the event were considered but for the incremental weighted mean only the samples until the respective time during the event were included in the computation.

$$C_E = \frac{\sum_{k=1}^{m} I_k \delta_k}{\sum_{k=1}^{m} I_k} \quad (5)$$

The focus of this study was not on the differences in the pre-event water contributions to streamflow due to the choice of the temporal weighing technique, as these have already been demonstrated (McDonnell et al., 1990). Instead, we use the different temporal weighing techniques to for comparison of the differences in the IHS results resulting from the spatial variability in the rainfall isotope composition to this well-known effect.

The effect of the different rain sampling locations on the IHS results was assessed by determining the pre-event water fractions in streamflow for WS04, WS10 and WS19 based on the incremental intensity mean (technique IV) for each of the eight rain samplers. While only a few of the rain samplers were located inside WS04, WS10 or WS19, we determined the pre-event water fractions for each of the rainfall sampling locations because it is common in small catchment studies to collect rainfall samples from a location near the catchment (e.g. in a nearby clearing). The uncertainty estimates of the pre-event water contributions to streamflow calculated with the incremental intensity mean (IV) were determined based on the method of Genereux (1998) and are given in Fischer et al. (2016).

3. RESULTS

3.1 Spatial variability in event total rainfall, rainfall intensity and the event weighted mean isotopic composition of rainfall

The spatial variability in event total rainfall, maximum rainfall intensity and weighted mean $\delta^{18}O$ of rainfall varied from event to event (Table 1 and 2, Figure 2). Events 3 and 5 had the highest event total rainfall and were characterized by large spatial differences in event total rainfall and maximum rainfall intensity (Figure 2c and e). The weighted mean $\delta^{18}O$ of rainfall for these events was only available for four rain samplers in the lower elevations because the rain changed to snow after peak discharge in the higher elevations zone was reached. Events 9 and 11 were smaller but were also characterized by a relatively large variability in event total rainfall (Figure 2g and i). The weighted mean $\delta^{18}O$ varied between -4.83 and -4. 25 ‰ for event 9 and between -9.06 and -7.35 ‰ for event 11 (Table 2, Figure 2g and 2i). Events 1, 6, 10 and 12 had smaller spatial differences in event total rainfall (coefficients of variation smaller than 0.1 and a range in event total rainfall smaller than 6 mm) and maximum rainfall intensities (Figure 2a, f, h and j). The differences between the minimum and maximum weighted mean $\delta^{18}O$ (i.e. *the spatial range of the weighted mean* $\delta^{18}O$*;* S_R) were 0.34, 0.88, 0.57, and 3.6 ‰ for events 1, 6, 10 and 12 respectively (Table 2, Figure 2a, f, h and j). For the smallest events (events 2 and 4), the range in event total rainfall was small (< 4 mm) but the range in the weighted mean $\delta^{18}O$ of rainfall (S_R) was 1.3 ‰ (Table 2, Figure 2b and d).

< Figures 2 and 3 here please >

The air masses for the investigated rainfall events originated from the North Atlantic Ocean and the Mediterranean (Table 1, Figure 3a and 3b). The majority of the collected rainfall samples fell on or just above the global meteoric water line (GMWL) (Figure 3c). The first samples of event 9 were slightly enriched in $\delta^{18}O$ and did not plot on the GMWL, indicating a potential below cloud evaporation effect.

Rain gauge TB-11 had a $M_{RD\,P}$ close to zero, which means that this was the most representative location for event total rainfall in the Zwäckentobel catchment (Figure 2k). Rain gauges TB-11 and TB-12 had a $M_{RD\,^{18}O}$ close to zero and were thus the most representative locations for the weighted mean $\delta^{18}O$ (Figure 2l). These results suggest that TB-11 can be considered the most representative measurement location for the entire Zwäckentobel catchment. However, the relative difference in $\delta^{18}O$ varied between -0.08 and 0.04 ‰ for TB-11 and between -0.09 and 0.12 ‰ for TB-12 for the different rain events, suggesting that these representative samplers may not be representative for all events.

The Pearson correlation coefficient was calculated for the relations between total rainfall, maximum rainfall intensity and elevation to examine whether the patterns in event total rainfall or maximum rainfall intensity were related to elevation. For event 4, 5 and 9, total rainfall was correlated ($r = 0.95$, 0.95 and 0.87 respectively) with rainfall intensity (Figure 4 and Table 4) but there was no significant correlation ($p < 0.05$) between event total rainfall, the maximum rainfall intensity or elevation for any of the other events (Figure 4 and Table 4). The weighted mean $\delta^{18}O$ of rainfall and was correlated with event total rainfall for event 12 ($r = 0.85$) and with maximum rainfall intensity for event 2 ($r = 0.81$; Figure 4 and Table 4). For the other events there was no significant correlation between the weighted mean $\delta^{18}O$ and event total rainfall or maximum rainfall intensity. The weighted mean $\delta^{18}O$ of rainfall was strongly negatively correlated to elevation for event 1, 2 and 12 ($r \approx -0.84$; Figure 4 and Table 4). Analyzing the weighted mean $\delta^{18}O$ of the rain samplers along the two main transects (T1 or T2, Figure 1b) or for two elevation classes (below and above 1350 m a.s.l.) resulted in statistically significant correlations between the weighted mean $\delta^{18}O$ of rainfall and event total rainfall, maximum rainfall intensity or elevation for some events (Table 4).

<Table 4 here please>

<Figure 4 here please>

The difference between the maximum and minimum weighted mean $\delta^{18}O$ for the different sampling locations (i.e. *the spatial range of the weighted mean* $\delta^{18}O$*;* S_R) increased slightly with increasing event total rainfall (up to 2.7 ‰) but was very variable for the large events (Figure 5). There was no statistical significant relation between the spatial range of the weighted mean $\delta^{18}O$ and the maximum rainfall intensity or event duration (Figure 5).

< Figure 5 here please >

3.2 Temporal variability in rainfall and its isotopic composition

Rainfall became more depleted in $\delta^{18}O$ during the events but the exact temporal pattern differed between the events (Figure 6). For events 2, 4 and 9, the $\delta^{18}O$ decreased by 1-2 ‰ from onset of rainfall towards the end of the events, for events 1, 6, 10 and 12, $\delta^{18}O$ decreased by 2-8 ‰, while for events 3, 5 and 11 it decreased by 4-11 ‰. The decrease in $\delta^{18}O$ was more variable for events 3, 5 and 11 than for events 2, 4 and 9, with sudden increases or decreases in $\delta^{18}O$ during the event. The mean of the difference maximum and minimum $\delta^{18}O$ measured during an event for the different rain samplers (i.e., *mean temporal range in* $\delta^{18}O$*;* M_{TR}) increased with increasing event total rainfall from 1 to 10 ‰ (Figure 5). There was no clear relation between the mean temporal range in $\delta^{18}O$ and the maximum rainfall intensity or event duration (Figure 5).

< Figure 6 here please >

The change in $\delta^{18}O$ of rainfall during the rainfall events was relatively similar for all eight sampling locations but there were differences between the different rain samplers (Figure 6). The spatial variability in $\delta^{18}O$ was relatively large during the first 5 mm of rainfall, with a standard deviation of 0.5-1.5 ‰ (Figure 7). The variability of the sampled $\delta^{18}O$ between the

different rain samplers decreased during the event for events 1, 2, 4, 6, 9 and 10 but increased throughout the event for events 3, 5, 11 and 12 (Figure 7).

< Figure 7 here please >

Comparing the mean temporal range in $\delta^{18}O$ (i.e. the difference between the event maximum and minimum $\delta^{18}O$ measured at the different rain samplers, M_{TR}) with the spatial range in the weighted mean $\delta^{18}O$ (i.e. the difference between the maximum and minimum weighted mean $\delta^{18}O$ for the different sampling locations, S_R) for the different events shows that for most events the temporal variability in $\delta^{18}O$ during the event was larger than the spatial variability in the weighted mean $\delta^{18}O$ (Figure 8). However, for the small events, the spatial variability in $\delta^{18}O$ was equal or half of the temporal variability in $\delta^{18}O$ (Figure 8). For the large events, the temporal range in $\delta^{18}O$ was larger than the spatial variability (Figure 8). The ratio of M_{TR} and S_R did not depend on the maximum rainfall intensity or the duration of the event (Figure 8).

< Figure 8 here please >

3.3 Effect of different temporal weighing techniques on isotope hydrograph separation results

The effect of the different weighing techniques to account for the temporal variability in the isotopic composition of rainfall (techniques I-IV) on the minimum pre-event water contribution to streamflow was analyzed for WS04, WS10 and WS19 for all events. For events 2, 9 and 10 the differences in the calculated minimum fractions of pre-event water between the four different temporal weighting techniques were small (≤ 0.1) but for the other events the differences in the minimum fractions of pre-event water were larger than 0.4 (Figure 9). For small and moderate events with a small difference between the event maximum and minimum $\delta^{18}O$ (small M_{TR}) and a large difference between the isotopic composition of event and pre-event water, the different weighing techniques had a small effect on the calculated minimum fraction of pre-event water in streamflow in WS04, WS10 and WS19 (Figure 11). The differences in the calculated minimum fraction of pre-event water

to streamflow increased when the variability in the isotopic composition of the rainfall during the event increased (increasing M_{TR}) and when the differences between the event and pre-event water composition decreased. For example, the use of the weighted mean and intensity mean (I and II) resulted in a very depleted event water composition for event 3, which resulted in large calculated pre-event water contributions (Figure 10). For the incremental mean and the incremental intensity mean (III and IV), the event water composition became more depleted throughout the event and the differences in the isotopic composition of event water, pre-event water and stream water composition were smaller, which resulted in smaller calculated pre-event water contributions to streamflow (Figure 10). The opposite effect was seen for the medium sized event 11. The weighted mean and intensity mean (I and II) resulted in a more depleted event water composition and a smaller difference between event water, pre-event water and stream water during the event, resulting in a much smaller pre-event water contribution than for the incremental mean and incremental intensity mean (III and IV, Figure 10).

< Figure 9 here please >

3.4 Effect of the location of the rain sampler on hydrograph separation results

For some events the minimum fraction of pre-event water was highly dependent on which rain sampler was used to characterize the event water, while this choice was less important for other events. (Figure 9). For example, for events 3 and 11 in WS04 the calculated pre-event fractions for the different rain samplers differed by up to 0.6 and 0.7, respectively (Figure 10) but for event 2 the differences in the pre-event water fractions were less than 0.1 (Figure 10). Generally, the range in the calculated minimum fraction of pre-event water was small (up to <0.2) for events for which the spatial variability in $\delta^{18}O$ in rainfall was small (small S_R) and the difference between event and pre-event water composition was large (Figure 11). The range in the calculated minimum fraction of pre-event water in streamflow was large (up to 0.6) for events with a large spatial variability in the isotopic composition of

rainfall and a small difference in the isotopic composition of event water and pre-event water (Figure 11). These differences in the pre-event water contributions to streamflow due the spatial variability of the isotopic composition of rainfall were larger than the spatial uncertainty of baseflow (Fischer et al., 2015) and the uncertainty in the hydrograph separation estimated by Fischer et al. (2016).

The choice of which rain sampler was used also determined whether IHS was possible or not. For event 3, the use of the rain sampler in the southern part of the Zwäckentobel catchment prevented the application of IHS in WS04. For other events, (e.g., event 6 in WS04), IHS was not possible when the local rain sampler was used but was possible when using neighboring rain samplers.

< Figure 10 here please >

To assess the relative importance of the spatial variability in the isotopic composition of rainfall on the IHS results, we compared the range in the calculated minimum fraction of pre-event water due to the choice of the location of the rain sampler to the range in the calculated minimum pre-event water composition due the different weighing techniques to account for the temporal variability in the isotopic composition of rainfall. For many of the small and moderate events the range in the minimum fraction of pre-event water due to the location of the different rain samplers was larger or equal to the range in the minimum fraction of pre-event water due to the use of different temporal weighing techniques (Figure 11). For large events, the change in $\delta^{18}O$ during the event was generally large (large M_{TR}) compared to the spatial variability in the isotopic composition of rainfall. This is reflected in the range in the minimum pre-event water contributions to streamflow. For example for event 5, the range in the calculated minimum fraction of pre-event water for the different sampling locations was one third of the range in the minimum pre-event water contribution to streamflow obtained from the different temporal weighing techniques. This suggests that even for large events for which the temporal variability in the isotopic composition is large compared to the spatial

variability, the spatial variability in the isotopic composition of rainfall still has a significant effect on the IHS results.

< Figure 11 here please >

4. DISCUSSION

4.1 Spatiotemporal variability in rainfall and rainfall isotopic composition

The observed spatial differences in total rainfall amount and the isotopic composition of rainfall were large, with differences in event total rainfall amount of 5 mm to more than 30 mm and differences in the weighted mean $\delta^{18}O$ of rainfall of 0.3 ‰ to more than 2 ‰ over distances of only 250 meter. These differences in rainfall amount and the weighted mean $\delta^{18}O$ of rainfall were larger than the uncertainty in the measured rainfall amounts (< 5 % error for the rain gauges), the precision of the isotope analysis ($\delta^{18}O$ < 0.1 ‰) and the observed variability in the isotopic composition of pre-event water (< 0.5 ‰ for $\delta^{18}O$; Fischer et al., 2015). The observed spatial variability in the isotopic composition of rainfall of the Zwäckentobel catchment was smaller than the 7 ‰ difference in $\delta^{18}O$ of precipitation measured by McGuire et al. (2005) for Lookout Creek. However, this is not surprising considering that the Zwäckentobel catchment is 100 times smaller than Lookout creek and the elevation differences in the Zwäckentobel catchment (1084-1656 m a.s.l.) are also smaller than those in the Lookout Creek (428-1620 m a.s.l.). Even though the isotopic composition of the rainfall was not correlated to elevation or rainfall amount for most events and varied over short distances, the observed variability across the entire Zwäckentobel catchment (maximum elevation difference of 600 m) was within the range of what can be expected based on a typical change in $\delta^{18}O$ of -0.2 ‰ per 100 m elevation or -2 ‰ per 100 mm of precipitation (Dansgaard, 1964; Holko et al., 2012; Kern et al., 2014), which lead to a difference in the isotopic composition of rainfall of ≈ 1 ‰. The lack of a clear relation between the isotopic composition of rainfall for the individual events and rainfall amount or elevation is contrary

to studies that attributed the spatial variability of the isotopic composition of rainfall to the amount effect (Dansgaard, 1964; Tappa et al., 2016) or elevation effect (Holko et al., 2012; Kern et al., 2014), and the event based measurements of McGuire et al. (2005) but was also described by Kennedy et al. (1986) for a 620 km^2 catchment in California.

The surrounding mountains and the complex topography of the study area (Figure 3b) affect the local atmospheric circulation. Even if the air masses of an event had a westerly trajectory, they could approach the catchment from the east, such as in event 2 (Figure 2b and Figure 3a). For longer events (such as events 3 and 5) the wind direction changed during the event. Mountains can influence rainfall formation (Roe, 2005) by rainfall enhancement or shading effects (Schäppi, 2013; Sevruk and Mieglitz, 2002), resulting in an absence of an amount effect or elevation effect in the isotopic composition of precipitation (Friedman and Smith, 1970). Therefore, it is likely that the interaction of atmospheric circulation and topography resulted in the heterogeneous pattern of rainfall amount and its isotopic composition at the event scale and are likely partly responsible for the lack of an amount effect or elevation effect for the isotopic composition of rainfall, even when events with a similar wind direction (events 6 and 9, events 4 and 10 and events 3 and 12, Table 4) were analyzed together.

Rainfall data were not corrected for potential systematic errors. However, typical wind induced errors for the observed wind speeds (2-8 %; Nešpor and Sevruk, 1999) are similar to the tipping bucket volume error and smaller than the observed differences in rainfall amount and intensities. Canopy interception can also alter the isotopic composition of rainfall. Differences between rainfall and the throughfall, e.g. up to 2 ‰ as were observed by Kato et al. (2013) in throughfall collected in a 100 m^2 forest plot compared to rain water collected in the open field in eastern Japan during a single rainfall event. The spatial variability in the isotopic composition of the rainfall sampled only in the open fields in the Zwäckentobel is comparable to the spatial variation in the isotopic composition of throughfall observed in a 60 m^2 plot in the H.J. Andrews Experimental Forest by Allen et al. (2015).

The number of rain samplers in the Zwäckentobel catchment study was smaller than the 38 bulk samplers used by McGuire et al. (2005) and those used in large scale (long term) studies (Schürch et al., 2003; Seeger and Weiler, 2014; Smith et al., 1979), but in terms of station density (three times larger than e.g., McGuire et al., 2005) and temporal resolution our study provided more detailed observations. We, therefore, argue that the added value of our study lies in the detailed information of the small-scale spatiotemporal variability in rainfall and the $\delta^{18}O$ of rainfall at the event scale. This variable pattern in the isotopic composition of rainfall suggests that the spatial variability has to be characterized for each event separately and that interpolation based on relationships with rainfall amount or elevation, particularly those that are based on only two gauges (e.g., Lyon et al., 2009) should be used carefully.

The sequential rain samplers also gave information about the spatial variability in the temporal changes in the isotopic composition of rainfall during the events. Rainfall became more depleted throughout the events (Figure 5), as observed by many other rainfall isotope studies (e.g. Berman et al., 2009; Lyon et al., 2009; McDonnell et al., 1990; Penna et al., 2014). Some of the individual events had a range in $\delta^{18}O$ and $\delta^{2}H$ as that is comparable to the long term monthly GNIP data from the nearest station (Bern or Grimsel, ≈ 60 km away), e.g. events event 2 and 3 ($\delta^{18}O$, -20 to -2 ‰) and a comparable range as the Swiss National Network for the Observation of Isotopes in the Water Cycle (NISOT, 1994-2001: $\delta^{18}O$, -20 to -2 ‰; Schürch et al., 2003). Munksgaard et al. (2012) similarly, observed that the temporal range in the isotopic composition of rainfall during an event can be as large as the range in the monthly mean isotopic composition of rainfall. The temporal variability in the isotopic composition of rainfall generally increased with total rainfall amount and event duration but was not correlated with rainfall intensity. The spatial variability in the isotopic composition of rainfall was relatively large during the first 5 mm of rainfall and then either decreased during the event or increased throughout the event (Figures 4 and 6), suggesting that a large part of the spatial variability was due to the differences in the first rainfall and that the

isotopic composition of the rainfall could either become more similar or more different throughout the event. For large events, such as event 3, the differences in $\delta^{18}O$ between the different rain samplers (as represented by the standard deviation) varied throughout the event largely due to rain bursts (i.e. it increased and decreased with increasing total rainfall; Figure 7).

4.2 Consequence of the spatiotemporal variability in event water composition on hydrograph separation results

Presently (i.e., 2016), it is common to sample rainfall throughout an event to be able to account for the temporal variation in the isotopic composition of the rainfall in IHS. This was confirmed for the Zwäckentobel catchment, where, especially for large and long events with occasional rain bursts, the use of the weighted mean and weighted intensity mean (i.e. inclusion of the isotopic composition of rainfall which had not yet fallen) resulted in a large error in IHS results. The development of field laser spectroscopes (Berman et al., 2009; von Freyberg et al., 2016) made a leap and makes it easier to better characterize the temporal variability in the isotopic composition of rainfall (and streamflow). However, it is still uncommon to sample rainfall at multiple locations in small catchment studies. Especially since Lyon et al. (2009) showed, using two different sampling locations for one event, that the calculated fractions of pre-event water in streamflow were very different for the two samplers. The eight sequential rain samplers used for the ten different events analyzed in this study gave a more detailed insight into the influence of the spatiotemporal variability in the isotopic composition of rainfall on the IHS results. The results of this study show that it is not only necessary to account for the temporal variability in the isotopic composition of rainfall to have robust IHS results, but that it is also necessary to account for the spatial variability in the isotopic composition of rainfall. The range in the calculated minimum fraction of pre-event water was small for small events, largely because of the small spatial variability in the isotopic composition of rainfall for these events (Figure 11). For events with a larger spatial

variability in the isotopic composition of the rainfall, the variability in the minimum fraction of pre-event water was large. The effect of the spatial variability in the isotopic composition of rainfall was particularly large for events for which the differences between the event water and pre-event water composition were small.

The IHS calculations using the data from several rain samplers allowed quantifying the uncertainty in the IHS results due to the spatial variability in the rainfall. For the majority of the studied events the variability on the computed minimum pre-event water fractions originating from using data from different rain samplers was up to three times larger than the variability originating from using different weighing techniques. In other words, the potential error by not accounting for temporal variation was clearly smaller than the potential error by not accounting for spatial variation. To minimize the error caused by the spatial variability in the isotopic composition of rainfall on IHS results, one could use the most representative rain sampler in the catchment (TB-11). Even though the differences in the minimum pre-event water fractions calculated based on the most representative rain gauge and those of WG-01 were relatively small for most events (difference f_{pe} < 10 %), they could be larger than 20 % during the event; Figure 9). To better account for the spatial variability of the isotopic composition of the rainfall, the weighted average isotopic composition of rainfall across the catchment can be used (e.g. Thiessen polygons or if the data allows more advanced geostatistical methods). Due to equipment failure, it was only possible to determine the average isotopic composition of the rainfall for the three sub-catchments for some of the small events for which the spatial variability in the isotopic composition of the rainfall was generally small and the effect of the spatial variability on the IHS results was also small. Therefore we could not test the effect of different weighing and interpolation methods on the calculated minimum pre-event water contributions to streamflow and this thus remains a subject for future research. Nevertheless, the results stress that the IHS assumption that the isotope signature of event water is constant in space (Buttle, 1994; Klaus and McDonnell,

2013) cannot be assumed to be always valid. It is, thus, necessary to sample rainfall at different locations, even in small headwater catchments for each event, to obtain reliable results on the event water contributions to catchment runoff. This is particularly necessary when IHS results for different events or different catchments are compared, as the minimum pre-event water contributions may be significantly influenced by the spatiotemporal isotopic composition of the rainfall.

CONCLUSIONS

Most IHS studies in small headwater catchments characterize the temporal variability in the isotopic composition of rainfall but ignore the spatial variability in precipitation and its isotopic composition across the catchment. We observed that for some events, the spatial variability in the isotopic composition of rainfall was almost as large as the temporal variability in the isotopic composition of rainfall and varied from event to event. For most events there was no relation between the isotopic composition of rainfall and total rainfall amount, rainfall intensity or elevation. This means that it is not possible to estimate the isotopic composition of the rainfall across the catchment for an event based on information on topography or rainfall amount. The observed spatial variability in the isotopic composition of rainfall significantly influenced the IHS results, particularly for events for which the spatial variability in the isotopic composition of rainfall was large and the difference between the event and pre-event water composition was small. The differences in the calculated minimum pre-event water contribution to streamflow based on data from the different rain samplers were as large as 60 %. This suggests that multiple rain samplers should be used to characterize the isotopic composition of event water when performing event-based IHS in the sub-catchments of Zwäckentobel at event time scale, and likely also for other small headwater catchments.

ACKNOWLEDGEMENTS

We thank all the people who helped in the field and the laboratory, particularly Ilaria Clemenzi, Michael Rinderer, Martin Šanda, Russel Smith, Stefan Plötner, Stephan Müller, Karl Steiner, Andrea Kolleger, Ellen Cerwinka, Sandra Pool, Sandra Schärer, Nadja Lavanga, Seraina Kauer, Jana Dusik, Paribesh Pradhan, Danthu Vu, Renato Winkler, Andrea Ruecker, Yves Götz, Annagreth Schuler, Werni Ruhstaller, Bruno Kägi, Claudia Schreiner, Michael Hilf, Sandra Röthlisberger and Ivan Woodhatch. We thank our colleagues from the WSL Mountain Hydrology Group, especially Manfred Stähli, for the collaboration in the Alptal and sharing the data of WS04. The editor, associated editor and two anonymous reviewers provided helpful comments, which helped to improve the manuscript. We also thank Oberallmeindkorporation Schwyz (OAK), the Department of Environment of the Canton of Schwyz and the municipality Alpthal for the good cooperation.

REFERENCES

Allen, S.T., Keim, R.F., McDonnell, J.J., 2015. Spatial patterns of throughfall isotopic composition at the event and seasonal timescales. J. Hydrol. 522, 58–66. doi:10.1016/j.jhydrol.2014.12.029

Araguás-Araguás, L., Froehlich, K., Rozanski, K., 2000. Deuterium and oxygen-18 isotope composition of precipitation and atmospheric moisture. Hydrol. Process. 14, 1341–1355. doi:10.1002/1099-1085(20000615)14:8<1341::AID-HYP983>3.0.CO;2-Z

Berman, E.S.F., Gupta, M., Gabrielli, C., Garland, T., McDonnell, J.J., 2009. High-frequency field-deployable isotope analyzer for hydrological applications. Water Resour. Res. 45, n/a-n/a. doi:10.1029/2009WR008265

Bowen, G.J., Good, S.P., 2015. Incorporating water isoscapes in hydrological and water resource investigations. Wiley Interdiscip. Rev. Water 2, 107–119. doi:10.1002/wat2.1069

Brown, V.A., McDonnell, J.J., Burns, D.A., Kendall, C., 1999. The role of event water, a rapid shallow flow component, and catchment size in summer stormflow. J. Hydrol. 217, 171–190. doi:10.1016/S0022-1694(98)00247-9

Burns, D.A., 2002. Stormflow-hydrograph separation based on isotopes: the thrill is gone — what's next? Hydrol. Process. 16, 1515–1517. doi:10.1002/hyp.5008

Buttle, J.M., 1994. Isotope hydrograph separations and rapid delivery of pre-event water from drainage basins. Prog. Phys. Geogr. 18, 16–41.

Dansgaard, W., 1964. Stable isotopes in precipitation. Tellus 16, 436–468. doi:10.1111/j.2153-3490.1964.tb00181.x

Delavau, C., Chun, K.P., Stadnyk, T., Birks, S.J., Welker, J.M., 2015. North American precipitation isotope (δ18O) zones revealed in time series modeling across Canada and northern United States. Water Resour. Res. 51, 1284–1299. doi:10.1002/2014WR016259

Draxler, R., Rolph, G., 2012. HYSPLIT–Hybrid Single Particle Lagrangian Integrated Trajectory Model [WWW Document]. NOAA Air Resour. Lab. Silver Spring, USA. URL http://ready.arl.noaa.gov/HYSPLIT.php (accessed 4.3.16).

Fischer, B.M.C., Rinderer, M., Schneider, P., Ewen, T., Seibert, J., 2015. Contributing sources to baseflow in pre-alpine headwaters using spatial snapshot sampling. Hydrol. Process. 29, 5321–5336. doi:10.1002/hyp.10529

Fischer, B.M.C., Stähli, M., Seibert, J., 2016. Pre-event water contributions to runoff events of different magnitude in pre-alpine headwaters. Hydrol. Res. doi:10.2166/nh.2016.176

Friedman, I., Smith, G.I., 1970. Deuterium Content of Snow Cores from Sierra Nevada Area. Science (80-.). 169, 467–470. doi:10.2307/1730266

Genereux, D., 1998. Quantifying uncertainty in tracer-based hydrograph separations. Water Resour. Res. 34, 915–919. doi:10.1029/98WR00010

Goodrich, D.C., Faurès, J.-M., Woolhiser, D.A., Lane, L.J., Sorooshian, S., 1995. Measurement and analysis of small-scale convective storm rainfall variability. J. Hydrol. 173, 283–308. doi:10.1016/0022-1694(95)02703-R

Hegg, C., McArdell, B.W., Badoux, A., 2006. One hundred years of mountain hydrology in Switzerland by the WSL. Hydrol. Process. 20, 371–376. doi:10.1002/hyp.6055

Holko, L., Dóša, M., Michalko, J., Kostka, Z., 2012. Isotopes of oxygen-18 and deuterium in

precipitation in Slovakia. ournal Hydrol. Hydromechanics 60, 265–276. doi:10.2478/v10098-012-0023-2

Hrachowitz, M., Bohte, R., Mul, M.L., Bogaard, T.A., Savenije, H.H.G., Uhlenbrook, S., 2011. On the value of combined event runoff and tracer analysis to improve understanding of catchment functioning in a data-scarce semi-arid area. Hydrol. Earth Syst. Sci. 15, 2007–2024. doi:10.5194/hess-15-2007-2011

Hughes, C.E., Crawford, J., 2012. A new precipitation weighted method for determining the meteoric water line for hydrological applications demonstrated using Australian and global GNIP data. J. Hydrol. 464–465, 344–351. doi:10.1016/j.jhydrol.2012.07.029

James, A.L., Roulet, N.T., 2009. Antecedent moisture conditions and catchment morphology as controls on spatial patterns of runoff generation in small forest catchments. J. Hydrol. 377, 351–366. doi:10.1916/j.jhydrol.2009.08.039

Jordan, J.P., 1994. Spatial and temporal variability of stormflow generation processes on a Swiss catchment. J. Hydrol. 153, 357–382. doi:10.1016/0022-1694(94)90199-6

Kato, H., Onda, Y., Nanko, K., Gomi, T., Yamanaka, T., Kawaguchi, S., 2013. Effect of canopy interception on spatial variability and isotopic composition of throughfall in Japanese cypress plantations. J. Hydrol. 504, 1–11. doi:10.1016/j.jhydrol.2013.09.028

Katsuyama, M., Yoshioka, T., Konohira, E., 2015. Spatial distribution of oxygen-18 and deuterium in stream waters across the Japanese archipelago. Hydrol. Earth Syst. Sci. 19, 1577–1588. doi:10.5194/hess-19-1577-2015

Kennedy, V.C., Kendall, C., Zellweger, G.W., Wyerman, T.A., Avanzino, R.J., 1986. Determination of the components of stormflow using water chemistry and environmental isotopes, Mattole River basin, California. J. Hydrol. 84, 107–140. doi:10.1016/0022-1694(86)90047-8

Kennedy, V.C., Zellweger, G.W., Avanzino, R.J., 1979. Variation of rain chemistry during storms at two sites in northern California. Water Resour. Res. 15, 687–702. doi:10.1029/WR015i003p00687

Kern, Z., Kohán, B., Leuenberger, M., 2014. Precipitation isoscape of high reliefs: interpolation scheme designed and tested for monthly resolved precipitation oxygen isotope records of an Alpine domain. Atmos. Chem. Phys. 14, 1897–1907. doi:10.5194/acp-14-1897-2014

Klaus, J., McDonnell, J.J., 2013. Hydrograph separation using stable isotopes: Review and evaluation. J. Hydrol. 505, 47–64. doi:10.1016/j.jhydrol.2013.09.006

Krupa, S. V, 2002. Sampling and physico-chemical analysis of precipitation: a review. Environ. Pollut. 120, 565–594. doi:http://dx.doi.org/10.1016/S0269-7491(02)00165-3

Laquer, F.C., 1990. Sequential precipitation samplers: A literature review. Atmos. Environ. Part A. Gen. Top. 24, 2289–2297. doi:http://dx.doi.org/10.1016/0960-1686(90)90322-E

Laudon, H., Hemond, H.F., Krouse, R., Bishop, K.H., 2002. Oxygen 18 fractionation during snowmelt: Implications for spring flood hydrograph separation. Water Resour. Res. 38, 10–40. doi:10.1029/2002WR001510

Lyon, S.W., Desilets, S.L.E., Troch, P.A., 2009. A tale of two isotopes: differences in hydrograph separation for a runoff event when using δD versus δ18O. Hydrol. Process. 23, 2095–2101. doi:10.1002/hyp.7326

Lyon, S.W., Desilets, S.L.E., Troch, P.A., 2008. Characterizing the response of a catchment to an extreme rainfall event using hydrometric and isotopic data. Water Resour. Res. 44. doi:10.1029/2007WR006259

McDonnell, J.J., Beven, K., 2014. Debates—The future of hydrological sciences: A (common) path forward? A call to action aimed at understanding velocities, celerities and residence time distributions of the headwater hydrograph. Water Resour. Res. 50, 5342–5350. doi:10.1002/2013WR015141

McDonnell, J.J., Bonell, M., Stewart, M.K., Pearce, A.J., 1990. Deuterium Variations in Storm Rainfall: Implications for Stream Hydrograph Separation. Water Resour. Re 26, 455–458. doi:10.1029/WR026i003p00455

McGuire, K., McDonnell, J., 2008. Stable Isotope Tracers in Watershed Hydrology, in: Stable Isotopes in Ecology and Environmental Science. Blackwell Publishing Ltd, pp. 334–374. doi:10.1002/9780470691854.ch11

McGuire, K.J., McDonnell, J.J., Weiler, M., Kendall, C., McGlynn, B.L., Welker, J.M., Seibert, J., 2005. The role of topography on catchment-scale water residence time. Water Resour. Res. 41, 1–14. doi:10.1029/2004WR003657

Menzel, L., Lang, H., Martin, R., 2007. Mean Annual Actual Evaporation 1973–1992. Hydrol. Atlas Switz.

Munksgaard, N.C., Wurster, C.M., Bass, A., Bird, M.I., 2012. Extreme short-term stable isotope variability revealed by continuous rainwater analysis. Hydrol. Process. 26, 3630–3634. doi:10.1002/hyp.9505

Nešpor, V., Sevruk, B., 1999. Estimation of wind-induced error of rainfall gauge measurements using a numerical simulation. J. Atmos. Ocean. Technol. 16, 450–464. doi:10.1175/1520-0426(1999)016<0450:EOWIEO>2.0.CO;2

Pellerin, B.A., Wollheim, W.M., Feng, X., Vörösmarty, C.J., 2008. The application of electrical conductivity as a tracer for hydrograph separation in urban catchments. Hydrol. Process. doi:10.1002/hyp

Penna, D., Stenni, B., Šanda, M., Wrede, S., Bogaard, T. a., Gobbi, A., Borga, M., Fischer, B.M.C., Bonazza, M., Chárová, Z., 2010. On the reproducibility and repeatability of laser absorption spectroscopy measurements for δ2H and δ18O isotopic analysis. Hydrol. Earth Syst. Sci. 14, 1551–1566. doi:10.5194/hess-14-1551-2010

Penna, D., van Meerveld, H.J., Oliviero, O., Zuecco, G., Assendelft, R.S., Dalla Fontana, G., Borga, M., 2014. Seasonal changes in runoff generation in a small forested mountain catchment. Hydrol. Process. 29, 2027–2042. doi:10.1002/hyp.10347

Rinderer, M., van Meerveld, H.J., Seibert, J., 2014. Topographic controls on shallow groundwater levels in a steep, prealpine catchment: When are the TWI assumptions valid? Water Resour. Res. 50, 6067–6080. doi:10.1002/2013WR015009

Roa-García, M.C., Weiler, M., 2010. Integrated response and transit time distributions of watersheds by combining hydrograph separation and long-term transit time modeling. Hydrol. Earth Syst. Sci. 14, 1537–1549. doi:10.5194/hess-14-1537-2010

Roe, G.H., 2005. Orographic precipitation. Annu. Rev. Earth Planet. Sci., Annual Review of Earth and Planetary Sciences 33, 645–671. doi:10.1146/annurev.earth.33.092203.122541

Schäppi, B., 2013. Measurement and analysis of rainfall gradients along a hillslope transect in the Swiss Alps. PhD- Thesis, ETH Zürich. doi:Diss. ETH No. 21084

Schürch, M., Kozel, R., Schotterer, U., Tripet, J.P., 2003. Observation of isotopes in the water cycle—the Swiss National Network (NISOT). Environ. Geol. 45, 1–11. doi:10.1007/s00254-003-0843-9

Seeger, S., Weiler, M., 2014. Reevaluation of transit time distributions, mean transit times

and their relation to catchment topography. Hydrol. Earth Syst. Sci. 18, 4751–4771. doi:10.5194/hess-18-4751-2014

Sevruk, B., Mieglitz, K., 2002. The effect of topography, season and weather situation on daily precipitation gradients in 60 Swiss valleys. Water Sci. Technol. 45, 41–48.

Sklash, M.G., Farvolden, R.N., Fritz, P., 1976. A conceptual model of watershed response to rainfall, developed through the use of oxygen-18 as a natural tracer. Can. J. Earth Sci. 13, 271–283. doi:10.1139/e76-029

Smith, G.I., Friedman, I., Klieforth, H., Hardcastle, K., 1979. Areal Distribution of Deuterium in Eastern California Precipitation, 1968–1969. J. Appl. Meteorol. 18, 172–188. doi:10.1175/1520-0450(1979)018<0172:ADODIE>2.0.CO;2

Tappa, D.J., Kohn, M.J., McNamara, J.P., Benner, S.G., Flores, A.N., 2016. Isotopic composition of precipitation in a topographically steep, seasonally snow-dominated watershed and implications of variations from the global meteoric water line. Hydrol. Process. 30, 4582–4592. doi:10.1002/hyp.10940

Tweed, S., Munksgaard, N., Marc, V., Rockett, N., Bass, A., Forsythe, A.J., Bird, M.I., Leblanc, M., 2016. Continuous monitoring of stream δ18O and δ2H and stormflow hydrograph separation using laser spectrometry in an agricultural catchment. Hydrol. Process. 30, 648–660. doi:10.1002/hyp.10689

Vachaud, G., Passerat De Silans, A., Balabanis, P., Vauclin, M., 1985. Temporal Stability of Spatially Measured Soil Water Probability Density Function. Soil Sci. Soc. Am. J. 49. doi:10.2136/sssaj1985.03615995004900040006x

Vitvar, T., Balderer, W., 1997. Estimation of mean water residence times and runoff generation by180 measurements in a Pre-Alpine catchment (Rietholzbach, Eastern Switzerland). Appl. Geochemistry 12, 787–796. doi:10.1016/S0883-2927(97)00045-0

von Freyberg, J., Studer, B., Kirchner, J.W., 2016. A lab in the field: high-frequency analysis of water quality and stable isotopes in streamwater and precipitation. Hydrol. Earth Syst. Sci. Discuss. 2016, 1–32. doi:10.5194/hess-2016-585

Xu, X., Guan, H., Deng, Z., 2014. Isotopic composition of throughfall in pine plantation and native eucalyptus forest in South Australia. J. Hydrol. 514, 150–157. doi:10.1016/j.jhydrol.2014.03.068

TABLES

Table 1 Hydrometeorological characteristics of the different sampled events: Difference in time of the initiation of rainfall initation betweenfor the first and last rain gauge to respond ($P_{start\ diff}$), and mean event duration (P_{length}), mean total rainfall ($P_{tot.}$), mean averagehourly rainfall intensity (I), the mean maximum hourly rainfall intensity (I_{max}) for all rain gauges, as well as the mean wind speed at WG-01 (U_W) and the maximum specific discharge at WS04 (Q_{peak}). The standard deviations are given in parentheses.

event nr.		1	2	3	4	5	6	9	10	11	12
year		2010				2011					
day-month		8 Sep	17 Sep	24 Sep	4 Oct	29 Jun	8 Jul	24 Aug	27 Aug	4 Sep	18 Sep
$P_{start\ diff}$	[h]	1.8	0.2	0	0	0	1.3	0.1	0.3	0	0.6
P_{length}	[h]	10 (0.15)	8 (0.5)	70 (1.1)	10 (0.2)	23 (1)	11 (0.8)	2 (0.7)	19 (.15)	24 (0.14)	11 (0.13)
$P_{tot.}$	[mm]	22 (2.6)	11 (1.4)	109 (16)	10 (1)	84 (19)	25 (1.5)	12 (2)	20 (1)	51 (11)	25 (2)
I	[mm h^{-1}]	2.2(0.3)	1.3 (0.2)	1.5 (0.2)	0.9 (0.1)	3.6 (0.9)	2.5 (0.2)	6.0 (1)	1.0 (0.1)	1.9 (0.4)	1.6 (0.2)
I_{max}	[mm h^{-1}]	4.5 (0.6)	2.3 (0.3)	7.6 (1.1)	2.4 (0.4)	18 (8.4)	9.0 (0.9)	10.0 (3)	7.3 (0.7)	7.0 (1.4)	6.0 (1.4)
U_W	[m s^{-1}]	1.6 (0.6)	0.9 (0.4)	1.3 (0.7)	3.2 (1.3)	1.3 (0.6)	1.6 (0.6)	0.7 (0.6)	1.9 (0.6)	0.7 (0.6)	1.2 (0.6)
Q_{peak}	[l s^{-1} km^{-2}]	353	106	1010	53	3004	390	86	334	589	504

Table 2 The number of samples (*m*), the maximum, mean and minimum $\delta^{18}O$ [‰] for the different rain samplers (rows) and the different events (columns), as well as the the number of rain sampling locations for which rainfall was collected throughout the entire event (n_{RG}), the slope (a) and intercept (b) of the linear relation between $\delta^{18}O$ and $\delta^{2}H$ (see figure 3c), the mean of the difference between the event maximum and minimum $\delta^{18}O$ measured at the different rain samplers (M_{TR}) and the difference between the maximum and minimum weighted mean $\delta^{18}O$ of rainfall for the different sampling locations (S_R) for each event. Differences in total rainfall resulted in different number of samples (m) for each sampling location and event.

event nr.	1	2	3	4	5	6	9	10	11	12
n_{RG}	7	8	4	8	4	8	6	6	6	6
WG-01 *m*		4	25	2	11	4	4	5	11	4
max		-4.60	-8.39	-7.82	-4.61	-6.89	-2.90	-5.39	-3.15	-4.37
mean		-5.35	-13.38	-8.17	-6.68	-7.91	-4.52	-6.89	-8.36	-7.77
min		-6.63	-16.41	-8.53	-9.35	-8.95	-5.27	-7.59	-13.33	-11.70
range		2.03	8.02	0.72	4.74	2.07	2.37	2.20	10.17	7.34
TB-01 *m*	5	3	12*	2		6				
max	-8.03	-5.52	-8.25	-7.43		-7.26				
mean	-10.48	-5.93	-13.77	-9.32		-8.71				
min	-11.86	-6.59	-20.21	-11.21		-9.42				
range	3.84	1.08	11.95	3.78		2.16				
TB-06 *m*	4	3	19	3	10	4	5	4	12	3
max	-8.32	-5.12	-8.87	-7.35	-4.61	-5.10	-2.36	-4.96	-3.75	-4.64
mean	-10.36	-5.5	-13.75	-8.15	-6.78	-8.16	-4.27	-6.74	-7.54	-8.05
min	-11.63	-5.73	-20.40	-8.70	-9.35	-9.33	-5.68	-7.52	-12.67	-11.88
range	3.31	0.60	11.53	1.35	4.74	4.23	3.32	2.56	8.92	7.24
TB-07 *m*	5	3	18	3		6	4	4	11	5
max	-8.05	-5.12	-10.12	-6.97		-4.84	-2.36	-4.96	-3.75	-4.25
mean	-10.34	-5.38	-13.70	-7.95		-7.91	-4.44	-6.74	-7.84	-6.87
min	-11.38	-5.5	-19.50	-8.50		-9.63	-5.68	-7.52	-12.67	-10.86
range	3.33	0.38	9.38	1.52		4.79	3.32	2.56	8.92	6.60
TB-09 *m*	5	4	9*	3		4		3	4*	5
max	-7.79	-6.02	-8.93	-8.62		-5.53		-5.26	-5.06	-4.83
mean	-10.65	-6.29	-13.51	-9.05		-8.54		-6.88	-9.06	-9.61
min	-12.03	-6.55	-15.30	-9.64		-10.14		-7.62	-13.28	-12.77
range	4.24	0.53	6.37	1.03		4.61		2.36	8.21	7.94
TB-10 *m*	5	3	5*	3	10	5	3	4	12	5
max	-8.13	-5.74	-8.88	-7.72	-5.30	-5.70	-3.16	-6.78	-5.35	-4.75
mean	-10.60	-6.46	-13.36	-8.53	-7.45	-8.32	-4.83	-7.32	-7.40	-7.80
min	-11.80	-7.87	-17.33	-9.06	-9.56	-9.66	-6.21	-7.59	-9.72	-10.90
range	3.67	2.13	8.45	1.34	4.26	3.97	3.05	0.81	4.37	6.14
TB-11 *m*	5	4	13*	3	11	4	3	3	4*	4
max	-8.31	-5.28	-8.94	-7.19	-4.83	-5.46	-3.32	-5.06	-5.31	-4.51
mean	-10.49	-6.07	-13.90	-8.05	-5.66	-8.46	-4.66	-9.06	-5.83	-7.36
min	-11.53	-7.51	-20.25	-8.64	-6.62	-9.87	-5.70	-13.28	-6.56	-11.83
range	3.21	2.23	11.31	1.45	1.79	4.42	2.38	0.70	1.25	7.32
TB-12 *m*	4	3	13*	2		6	3	4	9	
max	-9.12	-6.11	-10.62	-7.97		-5.32	-3.02	-6.19	-5.38	
mean	-10.67	-6.65	-14.24	-8.38		-8.79	-4.25	-7.01	-7.35	
min	-11.62	-7.69	-17.32	-8.80		-10.00	-4.98	-7.43	-9.16	
range	2.51	1.58	6.70	0.84		4.68	1.96	1.24	3.78	
a	7.3	8.1	8.7	8	8.1	6.7	2.1	7.3	7.7	8.4
b	7.4	12.8	21.7	8.8	11.3	0.5	-14	11.2	8.6	13.4
M_{TR}	3.44	1.32	9.35	1.50	3.88	3.86	2.73	1.78	8	7.10
S_R	0.34	1.31	0.39	1.37	1.79	0.88	0.57	0.57	1.71	2.74

*Sampling inconsistency due to sampler malfunctioning or solid precipitation.

Table 3 The number of streamflow water samples (n_S), the $\delta^{18}O$ [‰] of pre-event stream water (C_{pe}), and the maximum and minimum measured $\delta^{18}O$ [‰] of streamwater for the ten different events in the three headwater catchments.

Event	1	2	3	4	5	6	9	10	11	12
WS04 C_{pe}		-10.50	-10.40		-10.70	-8.45	-8.50	-8.51	-8.96	-9.01
n_s		23	46		23	15	10	20	26	29
$C_{s\,max}$		-9.59	-10.40		-7.03	-8.67	-8.51	-8.08	-8.3	-8.01
$C_{s\,min}$		-10.53	-12.94		-8.81	-9.73	-8.82	-9.23	-9.28	-9.07
WS10 C_{pe}	-10.64		-10.42	-10.70	-9.43		-10.24	-9.79	-8.95	-9.75
n_s	24		53	24	35		8	10	20	23
$C_{s\,max}$	-10.35		-10.42	-10.27	-7.38		-8.40	-8.27	-8.17	-8.65
$C_{s\,min}$	-10.79		-12.42	-10.88	-9.44		-10.24	-8.75	-9.52	-9.76
WS19 C_{pe}	-10.46	-10.19	-10.26	-11.30	-9.10	-8.90				-8.79
n_s	24	23	54	24	34	13				22
$C_{s\,max}$	-9.80	-8.92	-10.26	-10.35	-6.82	-8.55				-7.08
$C_{s\,min}$	-11.04	-10.46	-14.32	-10.89	-8.54	-8.75				-8.80

Table 4 **The Pearson correlation coefficient for the relation between the weighted mean $\delta^{18}O$ of rainfall and event total rainfall ($P_{tot.}$), maximum hourly rainfall intensity (I_{max}) or elevation (E) for the entire data set, individual transects (see Figure 1b for the location of the transects) or elevation zones (below and above 1350 m a.s.l.). --, -, o, + and ++ indicate a correlation of [-1 to -0.8], [-0.8 to -0.5], [-0.5 to 0.5], [0.5 to 0.8], and [0.8 to 1] respectively. Black and bold symbols indicate statistically significant correlations ($p < 0.05$). An asterisks (*) indicates no or limited ($m < 3$) data.**

event nr.		*1*	*2*	*3*	*4*	*5*	*6*	*9*	*10*	*11*	*12*
Rainfall											
$P_{tot.}$	I_{max}	+	+	o	**++**	**++**	o	**++**	+	o	+
$P_{tot.}$	E	o	o	o	o	+	o	o	o	o	**--**
I_{max}	E	o	o	o	o	+	-	o	o	o	o
$\delta^{18}O$											
All	P	o	o	--	o	+	o	o	o	+	**++**
	I_{max}	o	**++**	-	o	+	o	o	o	o	+
	E	**--**	**--**	o	o	o	-	o	o	o	**--**
T1	P	o	o	--	-	--	+	+	o	++	**++**
	I_{max}	o	+	-	-	**--**	++	o	o	++	+
	E	--	--	o	**--**	--	**--**	o	o	-	--
T2	P	**++**	+		++		o	o	o	o	o
	I_{max}	o	**++**	*	++	*	+	-	++	--	++
	E	--	**--**		-		**--**	+	-	++	o
E <1350 m a.s.l.	P	o	+	--	o	++	o	++	++	++	o
	I_{max}	o	++	++	o	++	o	+	+	++	o
	E	o	-	-	o	o	-	o	o	++	o
E >1350 m a.s.l.	P	o	++		--		--		o		
	I_{max}	-	**++**	*	--	*	--	*	++	*	*
	E	o	+		--		o		++		

FIGURES

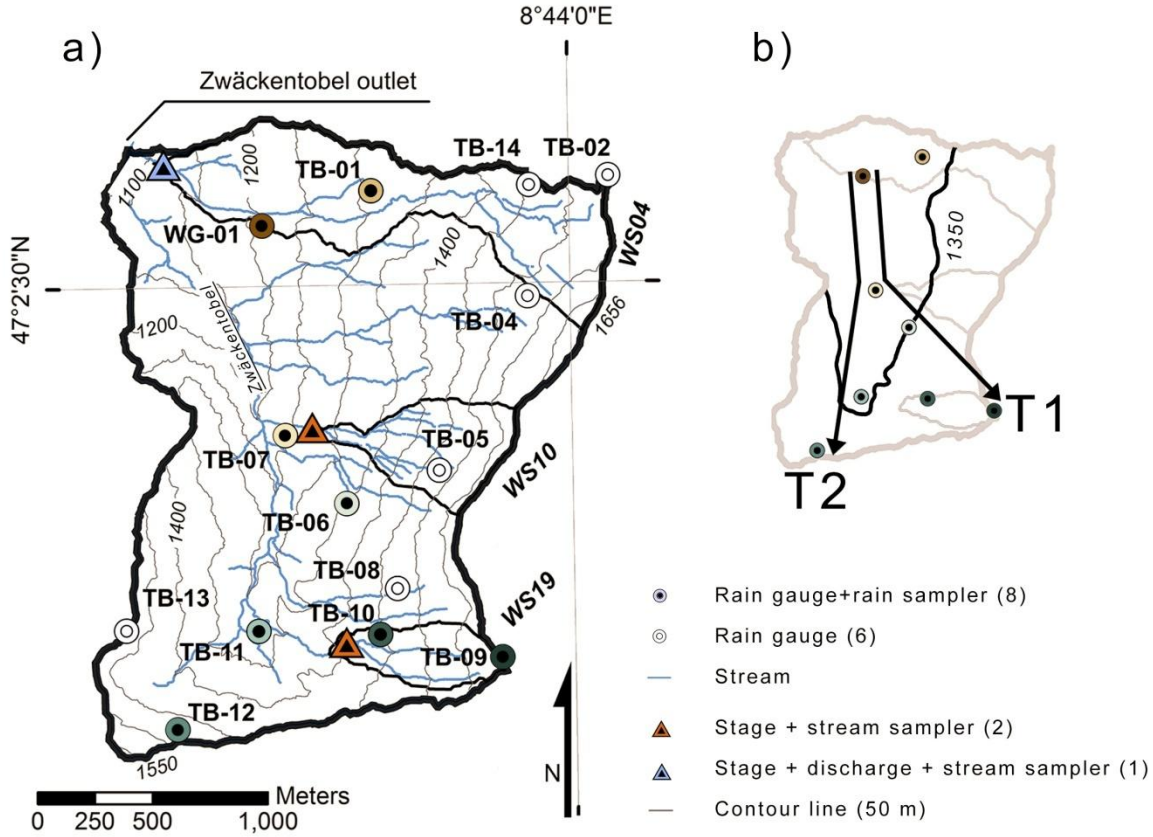

Figure 1 Map of the Zwäckentobel catchment with the WS04, WS10 and WS19 subcatchments, the location of the rain gauges, the rain samplers (the colors used for the different rain samplers are the same as in Figures 5, 9 and 10) and the stream sampling locations (a), and the two different transcects of the rain samplers (T1 and T2) and the contourline of 1350 m a.s.l. (b)

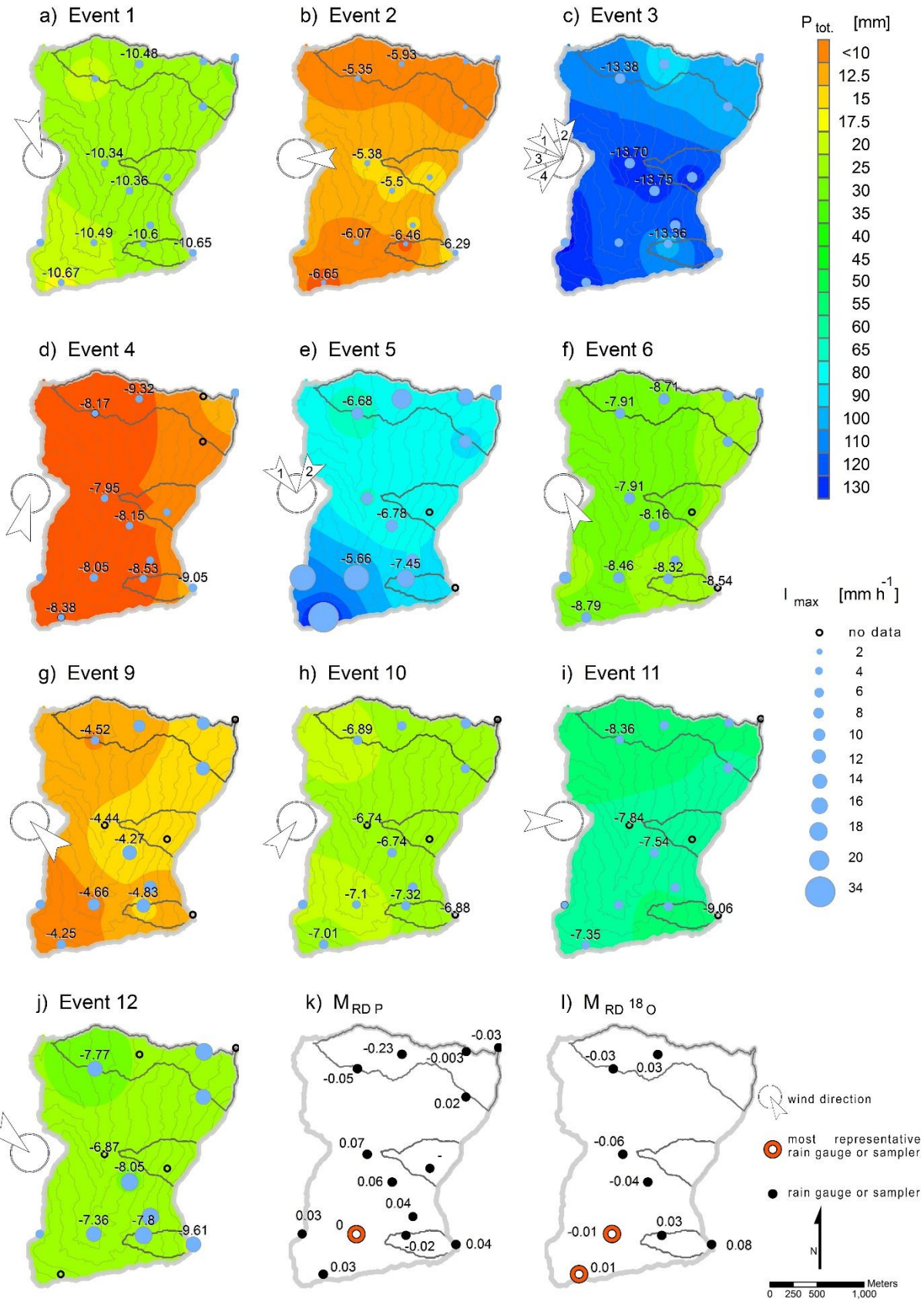

Figure 2 The spatial distribution event total rainfall ($P_{tot.}$ interpolated using inverse distance weighing) for the different events, with the 1-hour maximum rainfall intensity (symbol size) and the values of the weighted mean $\delta^{18}O$ of rainfall (values) (a-j), the mean relative difference of event total rainfall ($M_{RD\,P}$, k) and the mean relative difference of the weighted mean $\delta^{18}O$ of rainfall ($M_{RD\,18_O}$, l). The arrow indicates the direction of the main airmasses (similar to figure 3b), where the numbers indicate changes during the event, (in ≈ 12 hr periods). The rain gauge and samplers with the lowest M_{RD} are highlighted in red in figures k and l.

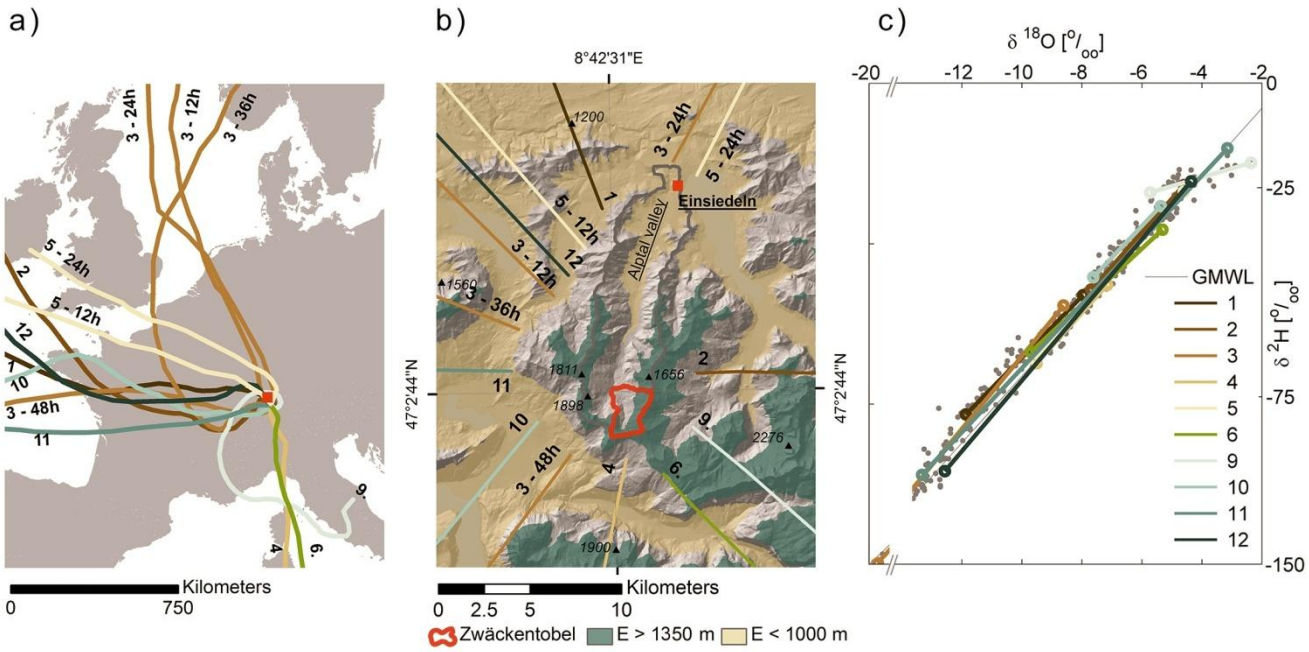

Figure 3 The trajectories of the airmasses for each event (indicated by bold number and different colors) calculated 96-h backwards using the HYSPLIT model (Draxler and Rolph, 2012) for the large scale (a) and regional scale (b), as well as the global meteoric water line (gray line) with all collected rainfall samples (gray circles) and streamwater samples for WG-01 with the linear regression line for each event (c). For the events 3 and 5, the trajectories of airmasses were calculated for 12 hour periods after the event started (indicated by event number - and the start of the 12 hour period). The dark green and ligth brown color in figure b indicate areas with elevations above 1350 m and below 1000 m respectively to highlight the complex topography) that affects the atmospheric flowpath.

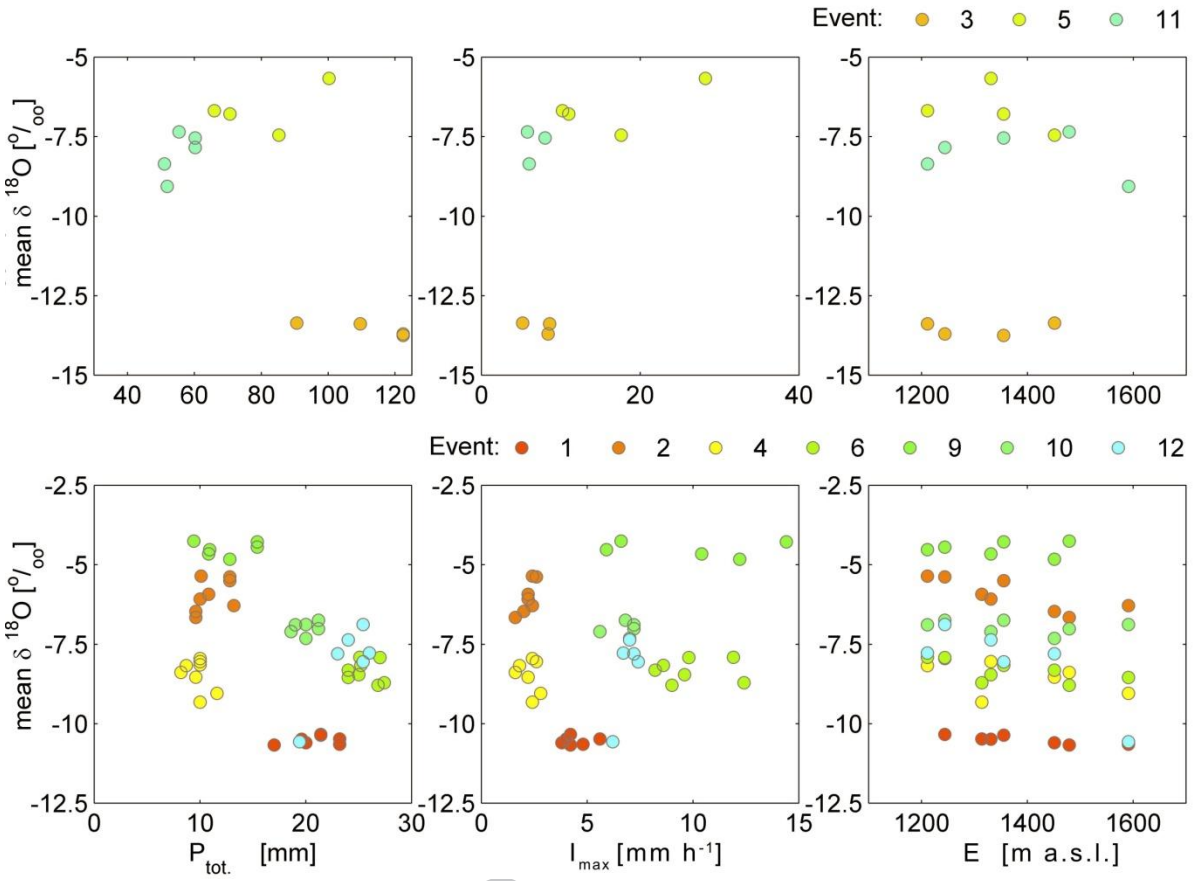

Figure 4 The weighted mean $\delta^{18}O$ of rainfall for each sampling location as a function of total rainfall amount ($P_{tot.}$), maximum rainfall intensity (I_{max}) and elevationt (E) for the different rainfall events (represented by the different colors). The top row shows the relations for the large events (> 30 mm) and the bottom row for small and medium events (< 30 mm).

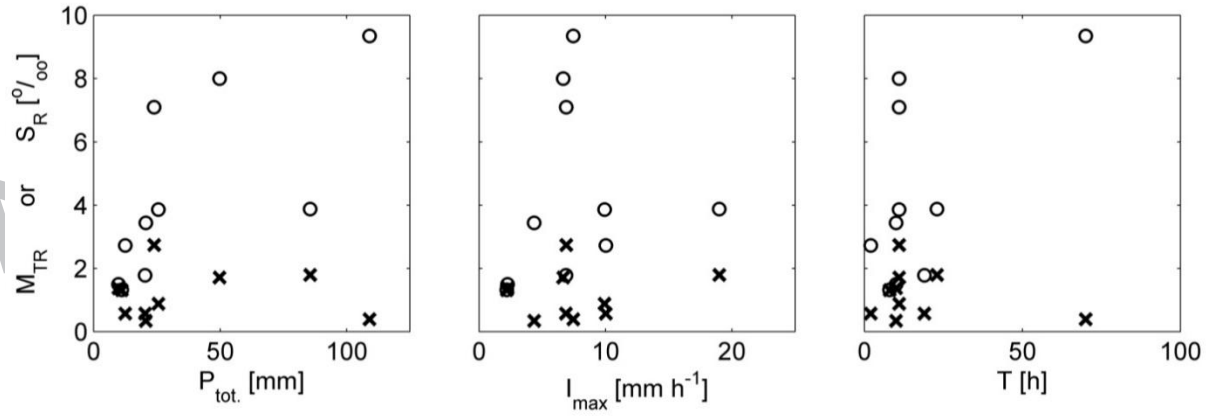

Figure 5 Mean temporal range (M_{TR}, circles) and spatial range (S_R, crosses) of $\delta^{18}O$ in rainfall for each event as a function of mean total rainfall ($P_{tot.}$), mean 1-hour maximum rainfall intensity (I_{max}) and event duration (T).

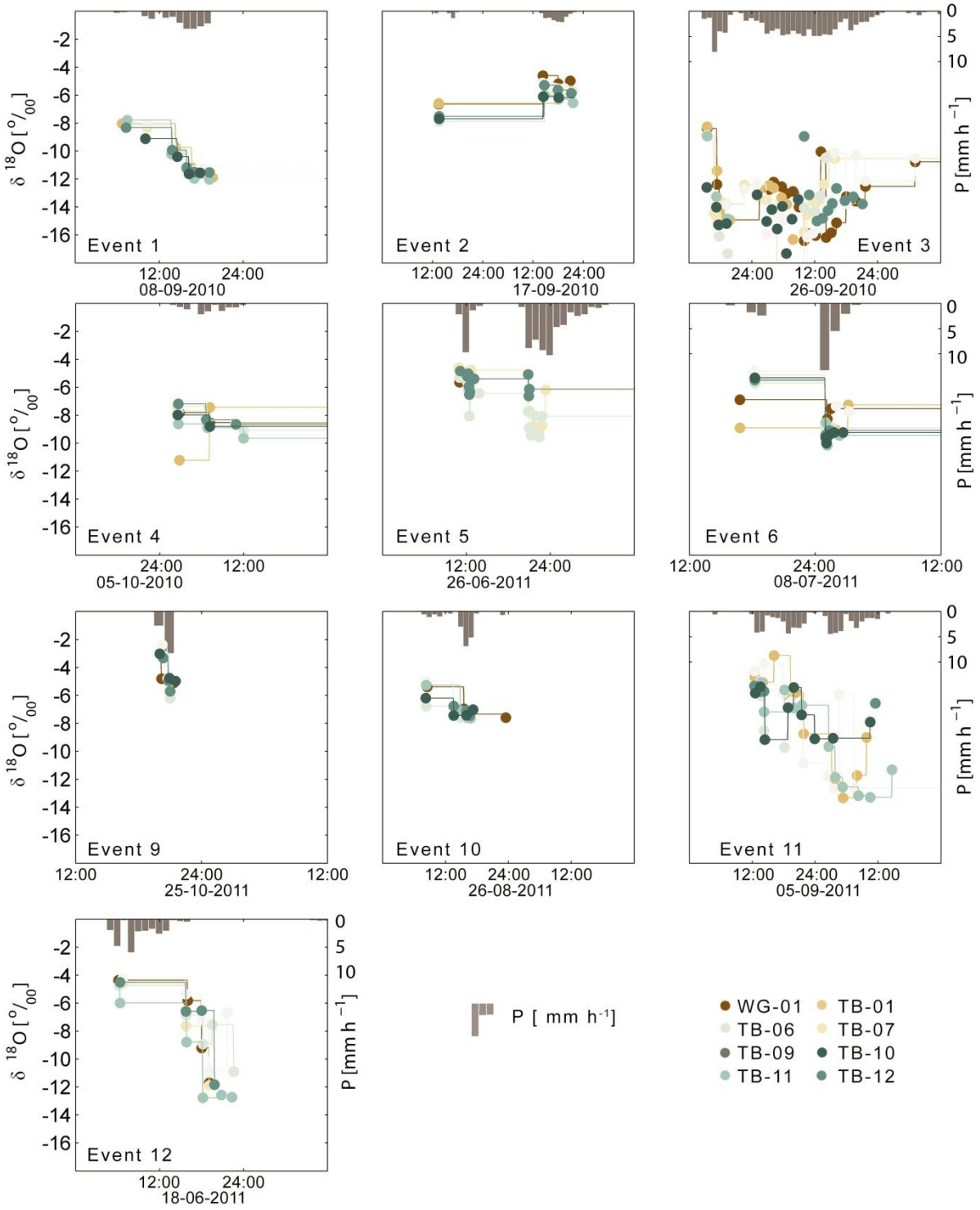

Figure 6 Rainfall intensity at WG-01 (bars) and the $\delta^{18}O$ of rainfall (5 mm increments) at the different rain samplers (circles) for the different events.

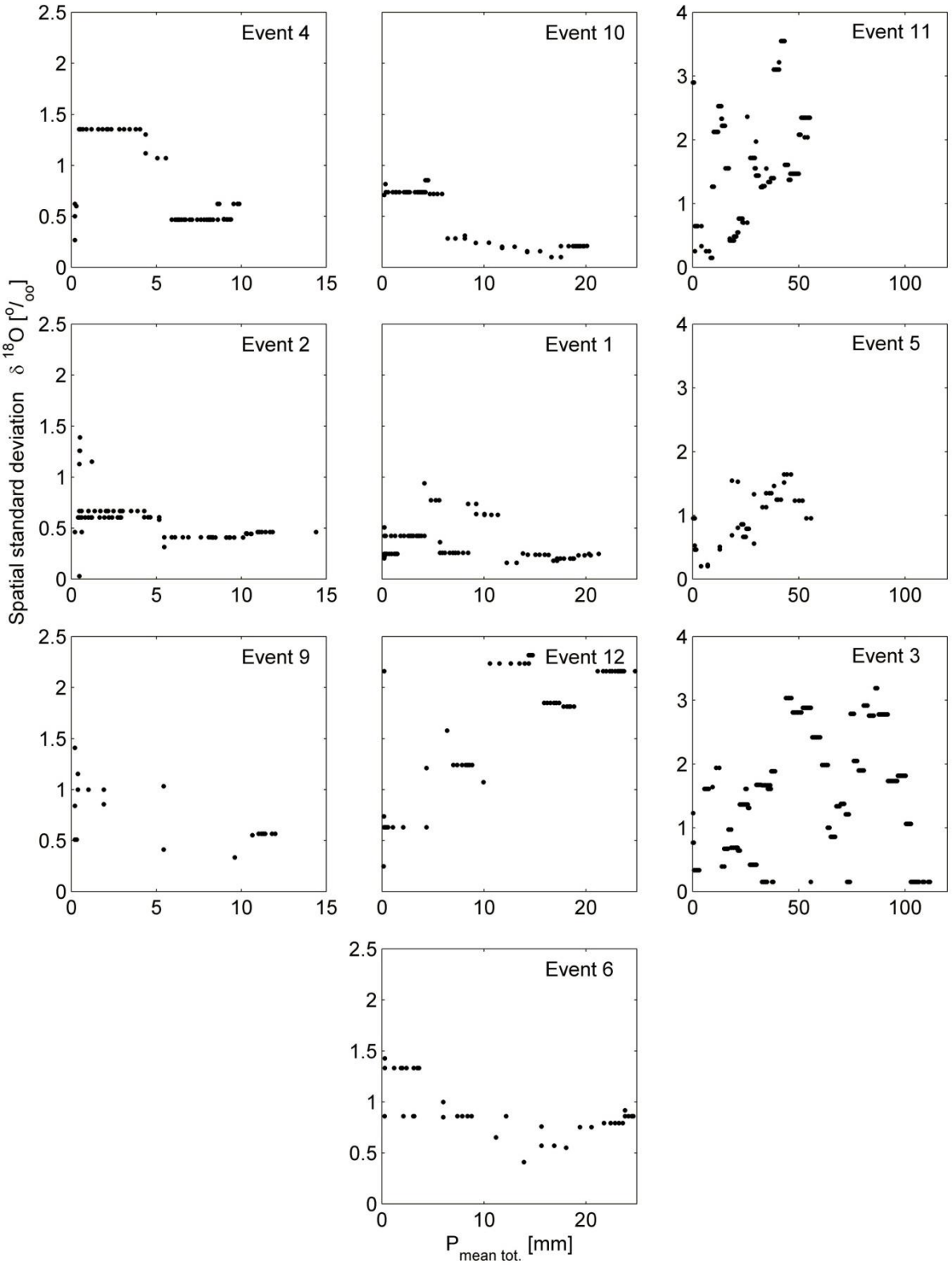

Figure 7 Spatial standard deviation of $\delta^{18}O$ in rainfall for the different events as a fuction of the cumulative mean rainfall ($P_{mean\ tot.}$) for the small events (left column), the medium sized events (middle column) and the large events (right column). Note that the y-axis for the large events is different and that a small part of the differences in the isotopic composition of the rainfall across the catchment is caused by the small differences in the time during which each 5 mm sample was collected (see Figure 6).

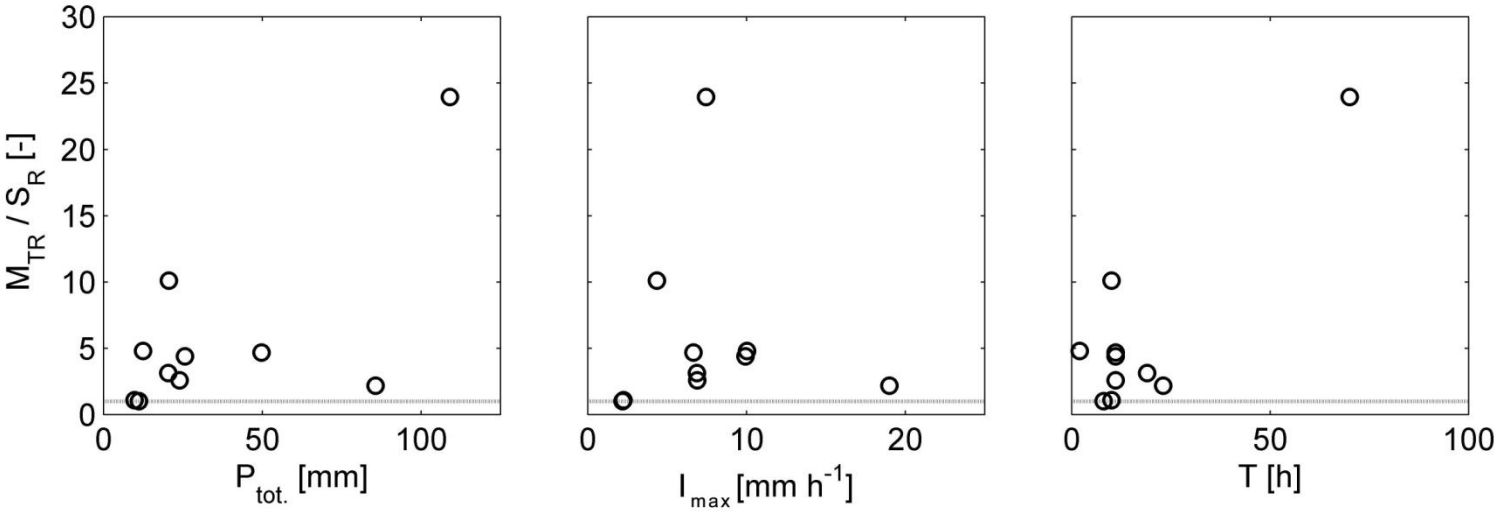

Figure 8 Ratio of the mean temporal range (M_{TR}) and the spatial range (S_R) of $\delta^{18}O$ in rainfall for each event as a function of mean event total rainfall ($P_{tot.}$), mean 1-hr maximum rainfall intensity (I_{max}) and event duration (T). The gray line represents a ratio of 1 (M_{TR} is equal to S_R).

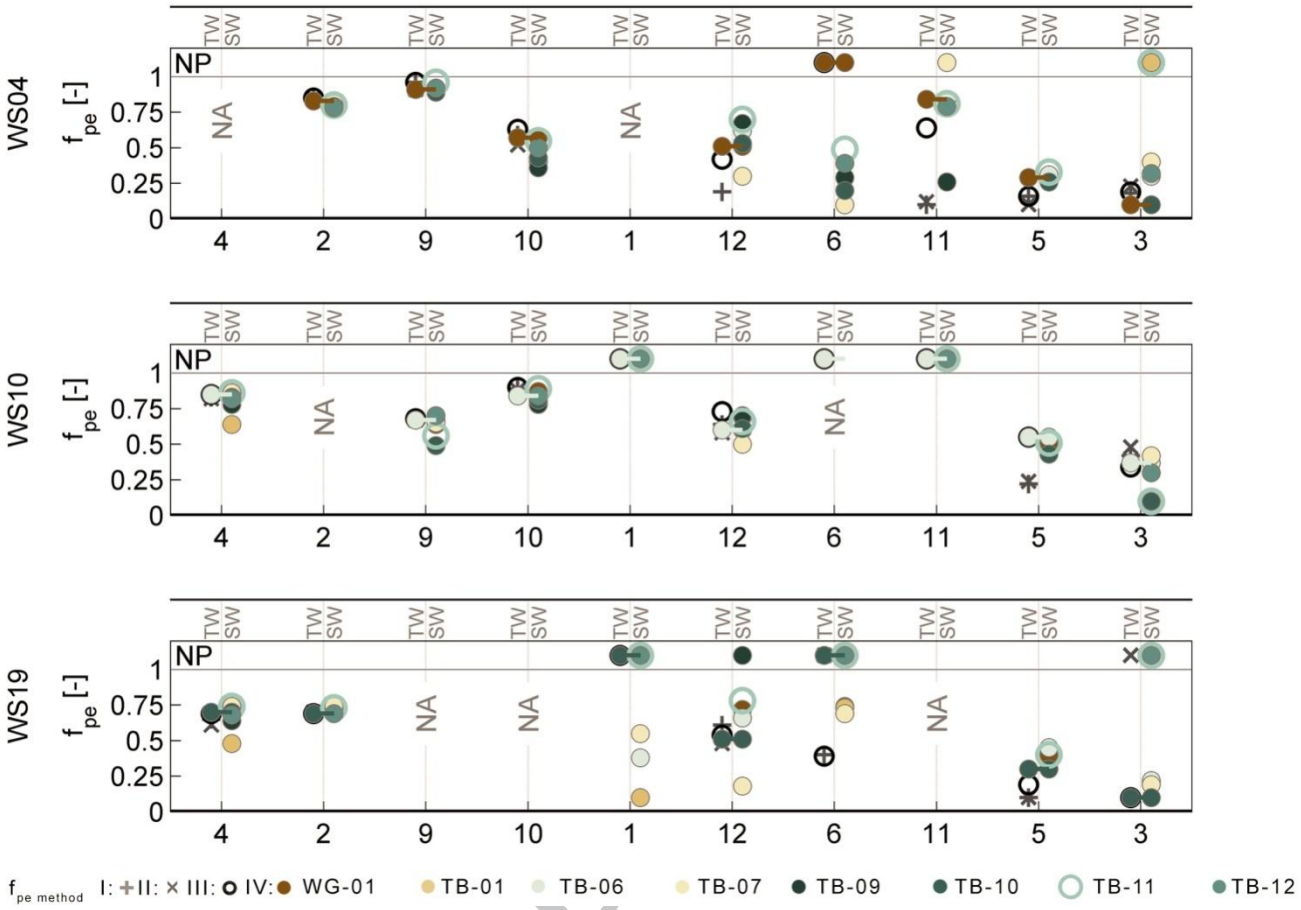

Figure 9 The minimum fraction of pre-event water for WS04 (top row), WS10 (middle row) and WS19 (bottom row) calculated for the different weighing techniques (I-IV) to account for the temporal variation in the isotopic composition of rainfall and the nearest rain sampler to the catchment (TW), and calculated with the incremental intensity mean for the different rainfall sampling locations (SW, different colored circles). The results of the most representative rain sampler TB-11 is shown with an open circle. The colored horizontal line connects the results for the incremental intensity mean for the nearest rain sampler (WG-01 for WS04, TB-6 for WS10 and TB-10 for WS19). NP indicates that hydrograph separation was not possible. NA indicates that the event was not sampled. The events are shown in order of increasing rainfall amount (see Table 1).

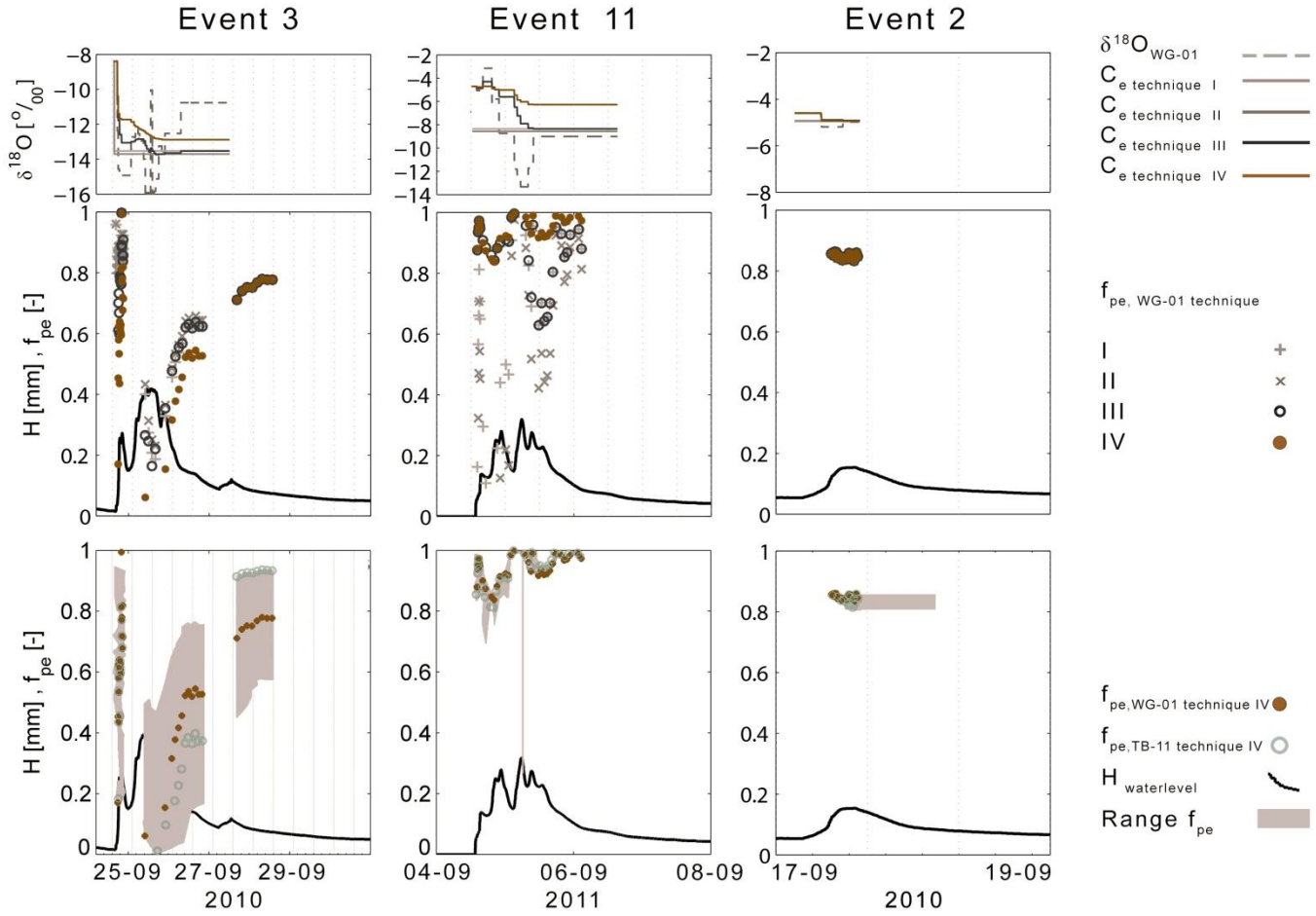

Figure 10 The isotopic composition of rainfall sampled at WG-01 (dashed line) and the calculated event water composition from WG-01 based on the four different temporal weighing techniques (C_e technique I-IV, top row), stream water level (black line) and the fraction of pre-event water obtained for the four different temporal weighing techniques in WS04 (middle row), and the range in the pre-event water contribution to streamflow calculated using the incremental intensity mean for the the different rainfall sampling locations (shading, lower row), the nearest rain sampler (WG-01; filled circles) and the most representative rain sampler TB-11 (open circles) for event 3 (left column), 11 (middle column) and 2 (right column).

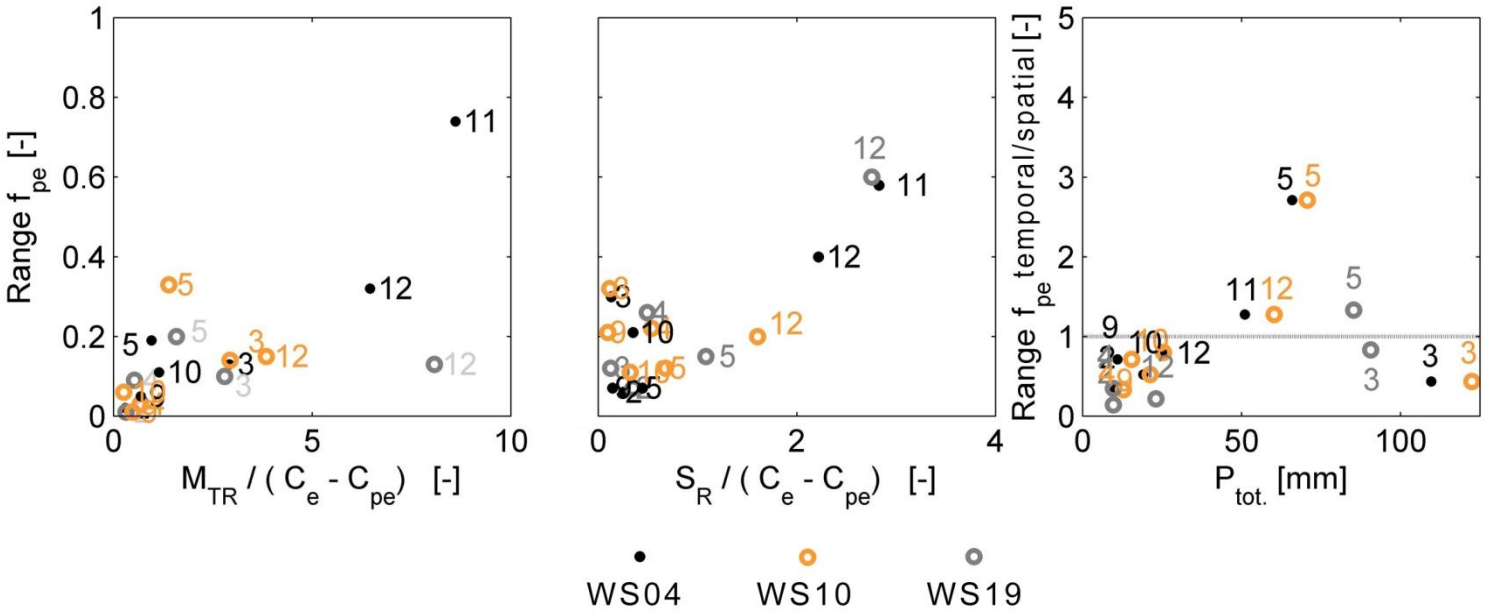

Figure 11 The range in the calculated minimum pre-event water contribution to streamflow for the different weighing techniques to account for the temporal variation in the isotopic composition of rainfall as a function of the ratio of the mean temporal range of $\delta^{18}O$ (M_{TR}) and the difference in the isotopic composition of event (C_e) and pre-event water (C_{pe}) (left panel), the range in the calculated minimum pre-event water contribution to streamflow based on the intensity weighted mean for the different rain samplers as a function of the ratio of the spatial range in $\delta^{18}O$ (S_R) and the difference in the isotopic composition of event and pre-event water (middle panel), and the ratio between the range in the minimum pre-event water contribution due to the different temporal weighing techniques and the range in the minimum pre-event water concentration due to different rain sampling locations as a function of event total rainfall ($P_{tot.}$, right panel) for WS04, WS10 and WS19 (black circles, open orange and open gray circles, respectively). The labels next to the symbol represents the event number.

- spatial variability in rainfall and its isotopic composition was high and differed for each event
- no relation between rainfall isotopic composition and rainfall characteristics or elevation
- spatial variability in rainfall isotopic composition affected isotope hydrograph separation